

Lumina-OmniLV: A Unified Multimodal Framework for General Low-Level Vision

Yuandong Pu^{1,2}, Le Zhuo², Kaiwen Zhu^{1,2}, Liangbin Xie^{3,4}, Wenlong Zhang²,
Xiangyu Chen^{2,6}, Peng Gao², Yu Qiao², Chao Dong^{4,5,2}, Yihao Liu^{2†}

¹Shanghai Jiao Tong University ²Shanghai AI Laboratory ³University of Macau
⁴Shenzhen Institutes of Advanced Technology, Chinese Academy of Sciences

⁵Shenzhen University of Advanced Technology

⁶Institute of Artificial Intelligence (TeleAI), China Telecom

† Corresponding Author

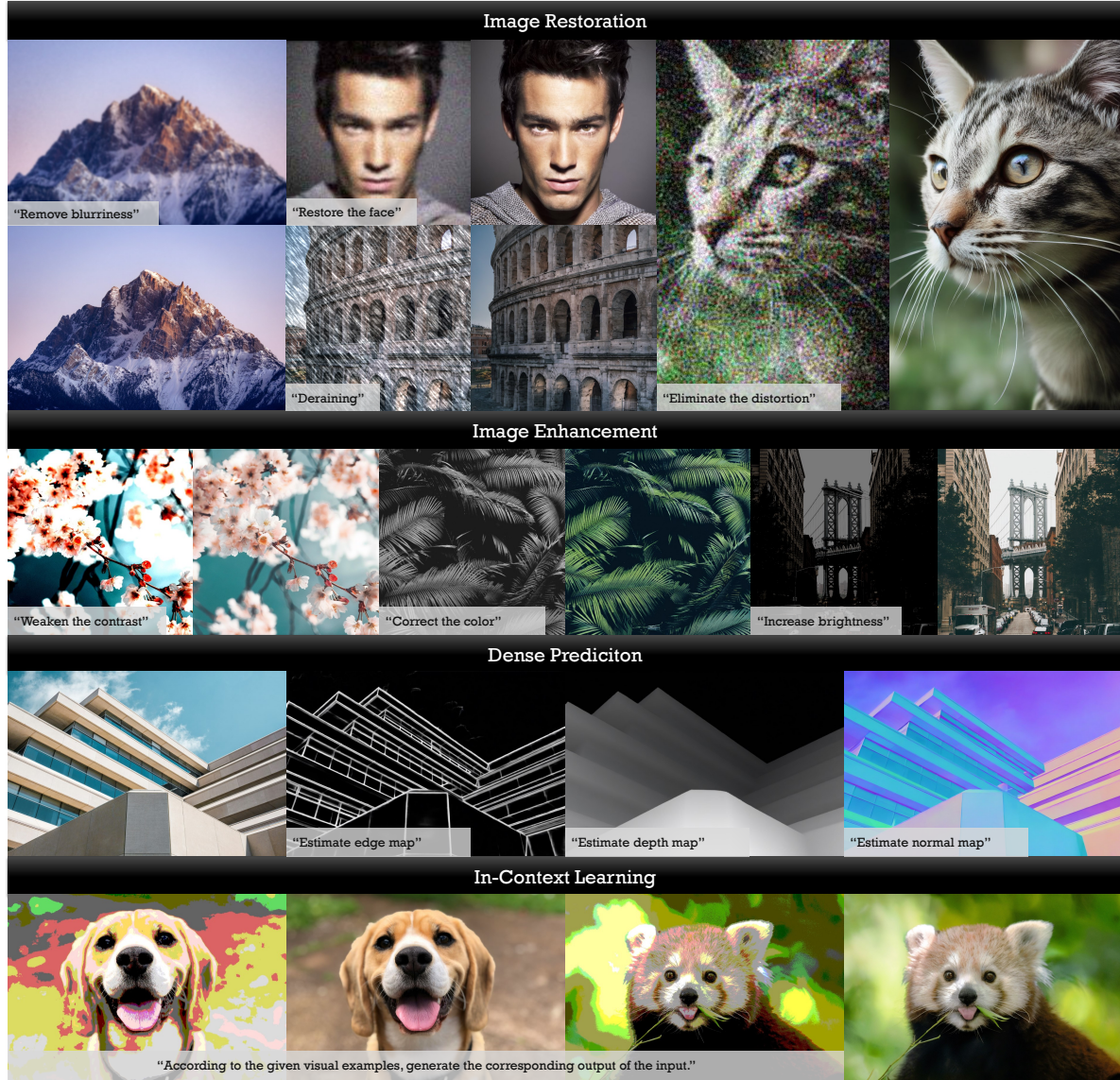


Figure 1. **Illustration of OmniLV's versatile capabilities.** As a universal framework, OmniLV is capable of handling a wide variety of low-level vision tasks within a single model, which adapts to diverse input-output domains and generates high-fidelity results.

Abstract

We present **Lunima-OmniLV** (abbreviated as **OmniLV**), a universal multimodal multi-task framework for low-level vision that addresses over 100 sub-tasks across four major categories, including image restoration, image enhancement, weak-semantic dense prediction, and stylization. **OmniLV** leverages both textual and visual prompts to offer flexible, user-friendly interactions. Built on Diffusion Transformer (DiT)-based generative priors, our framework supports arbitrary resolutions — achieving optimal performance at 1K resolution — while preserving fine-grained details and high fidelity. Through extensive experiments, we demonstrate that separately encoding text and visual instructions, combined with co-training using shallow feature control, is essential to mitigate task ambiguity and enhance multi-task generalization. Our findings also reveal that integrating high-level generative tasks into low-level vision models can compromise detail-sensitive restoration. These insights pave the way for more robust and generalizable low-level vision systems. The page of this project is [here](#).

1. Introduction

The rapid evolution of large-scale foundation models has revolutionized artificial intelligence, demonstrating remarkable generalization and multi-task capabilities across various domains. Unified frameworks such as GPT-4V [3], InternVL [25–27], Flamingo [8], OmniGen [98], and OneDiffusion [51] have showcased impressive performance by leveraging large-scale pretraining on multi-modal datasets. These models excel in semantic-driven high-level vision tasks, such as image classification, image understanding, visual generation and editing. In contrast, the development of unified models for low-level vision remains largely fragmented and underexplored.

Low-level vision encompasses a broad spectrum of tasks, including image restoration [21, 22, 29, 58, 106, 111], image enhancement [15, 19, 20, 90, 109], style transfer [35, 39], and weak-semantic dense prediction [48, 80, 101] (e.g., edge detection, depth estimation, normal map estimation). Unlike high-level vision tasks that rely on predefined semantic understanding, most low-level vision tasks do not require explicit object-level reasoning. Instead, they focus on pixel-level fidelity, fine-grained texture reconstruction, and feature extraction. This distinction makes the unification of low-level vision tasks particularly challenging, as different tasks often operate in vastly different output domains.

Existing approaches to low-level vision remain limited in generalization, usability, and scalability. Task-specific models [21, 53] are designed to handle a single task (e.g., denoising, deblurring, super-resolution), requiring extensive model redesigning and retraining to adapt to new tasks.

All-in-one restoration models, such as AirNet [53], PromptIR [75], and OneRestore [36], integrate multiple restoration tasks within a single framework, yet remain restricted to in-domain restoration, unable to generalize to cross-domain tasks such as feature extraction or style transfer. Visual-prompt-based models, such as PromptGIP [63] and GenLV [23], extend to cross-domain tasks using image prompt pairs, but require carefully crafted prompts, making them less intuitive and user-friendly compared to text-driven interaction. Furthermore, many existing methods operate only on fixed-resolution images, severely limiting their flexibility and real-world applicability. To summarize, high-resolution image processing still remains challenging, leaving ample room for improvement in task adaptability.

Given the inherent complexity and diversity of low-level vision, developing a truly universal model must handle multiple task domains while reliably preserving fine-grained details and high fidelity. A key requirement for such a model is flexible interaction mechanisms. While text-based instructions offer a convenient and intuitive way to specify tasks (e.g., “remove noise from this image”, “enhance brightness”, and “estimate the Canny edge”), certain tasks — such as style transfer — are difficult to define using text alone. Visual prompts, provided in the form of exemplar image pairs, provide an effective alternative by allowing the model to infer complex, task-specific transformations through visual analogy. Thus, an ideal general low-level vision model should integrate both textual and visual prompts for versatile and user-friendly task execution.

To address these challenges, we propose **OmniLV**, a universal multimodal multi-task framework for low-level vision, capable of handling over 100 sub-tasks via both textual and visual prompts. Built on Diffusion Transformer (DiT)-based generative priors [32, 38, 74, 83], our model significantly improves generalization and output quality across tasks. Fig. 1 presents the versatile capabilities of OmniLV. Unlike prior models constrained to fixed resolutions, our framework supports arbitrary resolutions, achieving optimal performance at 1K resolution. We systematically explore multimodal fusion strategies and propose a simple yet effective design that prevents task misinterpretation issues.

Throughout the development of OmniLV, we have gained several key insights that shape the design of a robust and generalizable low-level vision model. First, we find that separately encoding text-based and visual instructions is crucial for preventing task ambiguity, as naive fusion can lead to task misinterpretations (Sec. 3.1.2). Additionally, co-training the base model with shallow feature control proves to be an effective strategy for enhancing multi-task generalization (Sec. 3.1.3). Furthermore, incorporating high-level generative or editing tasks into a low-level vision model significantly compromises fidelity, particularly in detail-sensitive restoration tasks (Sec. 4.2). These find-

ings highlight the need for dedicated multimodal architectures tailored for low-level vision tasks.

In summary, our work makes the following key contributions. (1) We present the first unified multimodal framework capable of handling four major low-level vision categories (over 100 sub-tasks) through both text and image interactions. (2) We introduce an effective multimodal fusion mechanism that aligns text and image prompts, mitigating task misalignment issues. (3) We provide new empirical insights into the challenges of building multi-task low-level vision generalists, revealing how the integration of high-level generative and editing tasks can adversely impact fidelity-critical restoration tasks.

2. Related Work

2.1. Image Restoration with Generative Prior

Diffusion-based methods have emerged as a robust framework for image restoration, converting degraded inputs into high-quality outputs through reverse denoising. Several key works illustrate the versatility of this approach [7, 16, 58, 88, 97, 102, 106, 108]. StableSR [88] leverages the generative priors of pre-trained text-to-image diffusion models for blind super-resolution, employing a time-aware encoder and feature wrapping to balance quality and fidelity while accommodating arbitrary resolutions. DiffBIR [58] uses a two-stage pipeline where the first stage reduces degradations and the second stage employs a latent diffusion model (IRControlNet) to generate missing details, proving effective in denoising and face restoration. PASD [102] extends the Stable Diffusion framework for realistic super-resolution and personalized stylization by integrating a pixel-aware mechanism that improves both resolution precision and style adaptability. SUPIR [106] scales up large diffusion models such as StableDiffusion-XL, incorporating a trained adapter and a massive high-resolution dataset to enable text-guided, photo-realistic restoration in complex scenes. However, the limitation of these approaches is that they are confined to image restoration tasks and cannot address other challenges in low-level vision.

2.2. All-in-one Generative Models

Developing all-in-one models is an exciting yet challenging pursuit. In the realm of image generation, various studies have sought to build versatile systems [37, 50, 57, 70, 94, 98]. For example, OmniGen [98] encodes text and images into a unified tensor, utilizing causal attention for text tokens and bidirectional attention for image tokens. Pixwizard [57] introduces task-specific embeddings for image editing and understanding, while ACE [37, 70] offers a conditioning module that accepts diverse input images and processes them concurrently with a transformer. Additionally, UniReal [24] employs a video generation framework that treats images as individual frames, providing a universal solution for various image generation and editing tasks.

Despite these advances, most of these approaches focus on image generation and editing, leaving universal models for low-level vision relatively unexplored. Visual prompt-based approaches [23, 63] tackle cross-domain tasks by utilizing pairs of image prompts. However, their dependence on meticulously crafted prompts renders them less intuitive and user-friendly compared to text-driven alternatives. Moreover, many current methods are restricted to fixed-resolution outputs, limiting their practical applicability.

3. Method

3.1. Building OmniLV Step-by-Step

In this section, we detail the key design choices and learned insights in developing a universal low-level vision model, outlining our step-by-step thinking process.

3.1.1. Selecting the Base Model

Unlike most foundational image restoration models [32, 38, 74, 83] that are trained from scratch using deterministic regression objectives, we leverage a pre-trained text-to-image diffusion model as a strong initialization. Pre-trained diffusion models [32, 34, 49, 99, 117], trained on billions of images, offer rich visual priors that enhance generalization, support diverse resolutions and aspect ratios, and effectively capture the uncertainty inherent in multi-task image restoration. These properties allow us to build a more robust and versatile low-level vision model.

For our base model, we initialize with Lumina-Next [34, 117], a flow-based diffusion transformer that introduces several architectural improvements over traditional DiT-based models [74], including 2D Rotary Positional Encoding, QK Normalization, and Sandwich Normalization. Additionally, Lumina-Next adopts a flow-matching formulation, which improves training stability and accelerates convergence. To adapt this model for general low-level vision, we introduce a condition adapter that integrates low-quality inputs to enable effective task conditioning, which is illustrated in subsequent sections. The modified model is trained using a flow-matching loss to learn a conditional time-dependent velocity field, facilitating the transformation between noisy and clean image distributions. Please refer to the Supplementary for details of training loss.

3.1.2. Encoding Multimodal Information

Given an input image x , our goal is to generate the target image using both textual instructions and in-context visual exemplars. We explore two different encoding strategies: (1) **Separate encoding**, where text prompts are processed using a large language model (LLM), while visual exemplars are encoded independently. (2) **Unified encoding**, where both text and visual inputs are fused within a multimodal language model (MLLM). Fig. 2 illustrates the architectural differences between these two approaches. While unified encoding benefits from parameter efficiency

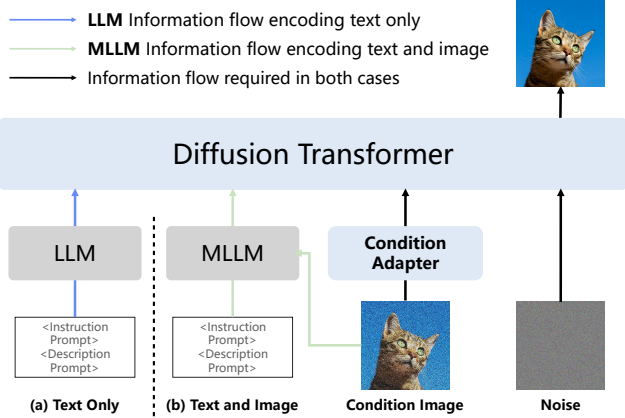
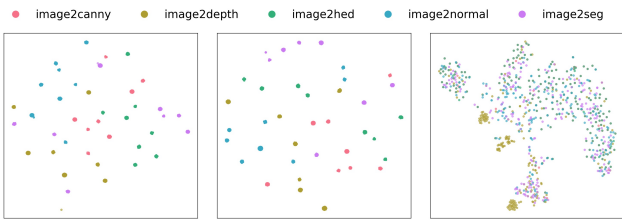


Figure 2. Comparison between MLLM guided and LLM guided framework.

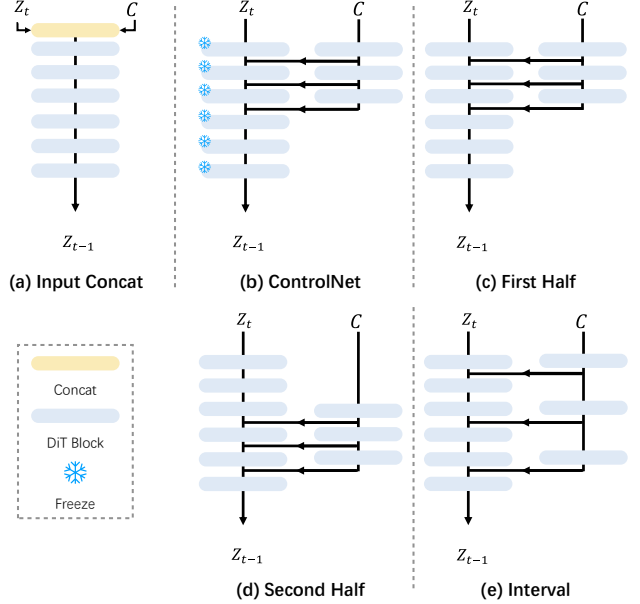


Position	Train DM?	SIDD		RealBlurJ		SR	
		PSNR↑	MUSIQ↑	PSNR↑	MUSIQ↑	PSNR↑	MUSIQ↑
(a) Input	✓	32.40	21.91	22.98	51.66	22.89	56.89
(b) First Half	✗	25.52	23.53	22.28	44.41	21.11	50.44
(c) First Half	✓	34.09	23.96	24.05	57.42	22.93	56.72
(d) Second Half	✓	29.60	23.38	23.15	54.35	22.96	56.60
(e) Interval	✓	34.07	23.06	22.77	53.50	22.80	56.38

Table 1. Ablation study on condition integration.

and leverages cross-modal correlations, we observe that it introduces critical limitations especially when applied to dense prediction tasks. Specifically, multimodal encoders often misinterpret task instructions, leading to inconsistencies in generated outputs. To better understand this issue, we visualize the encoded feature distributions in Fig. 3. Our findings indicate that mixing text and image prompts within a single encoder leads to severe task ambiguity. Since visual tokens dominate the shared feature space, text-based instructions often get overshadowed, leading to misalignment and incorrect outputs, as shown in Fig. 10.

Based on these observations, we adopt a separate encoding strategy: text instructions are processed via an LLM, while image exemplars are encoded using a visual VAE. This ensures clearer task separation, preventing interference between textual and visual guidance, and improves task accuracy across a vast number of low-level vision tasks.



3.1.3. Design Choices of Condition Integration

Integrating condition images into diffusion models is commonly achieved through two primary approaches: (1) **Feature Injection**: A trainable adapter injects feature maps into a frozen diffusion model [72, 113]. (2) **Input Concatenation**: Condition images are concatenated with inputs, and the entire model is fine-tuned. These designs have been widely used in in-domain single task (e.g. image restoration, canny2image), achieving remarkable results [58, 106]. To systematically investigate condition integration strategies for general low-level vision tasks, we conduct comparative experiments evaluating different design choices (see Fig. 4). Our findings, summarized in Tab. 1, are as follows: (1) Training only the adapter is suboptimal (settings (b) & (c)), indicating that fine-tuning the base model is necessary for adapting generative priors to diverse low-level tasks. (2) While input concatenation is efficient(setting(a)), adding additional parameters to process the condition image enhances performance (setting (c)), suggesting that explicitly modeling condition images helps extract more relevant structural and contextual information. (3) The injection position significantly influences the performance (settings (c), (d), & (e)). Integrating condition information in the first half of the network leads to better results, likely because early-stage modulation ensures stronger feature guidance throughout the process.

Based on these findings, we propose a co-training condition adapter, which jointly optimizes the adapter and base model. Unlike ControlNet-like architectures, which keep the base model frozen, our approach ensures deeper feature alignment, improving multi-task generalization and fidelity.

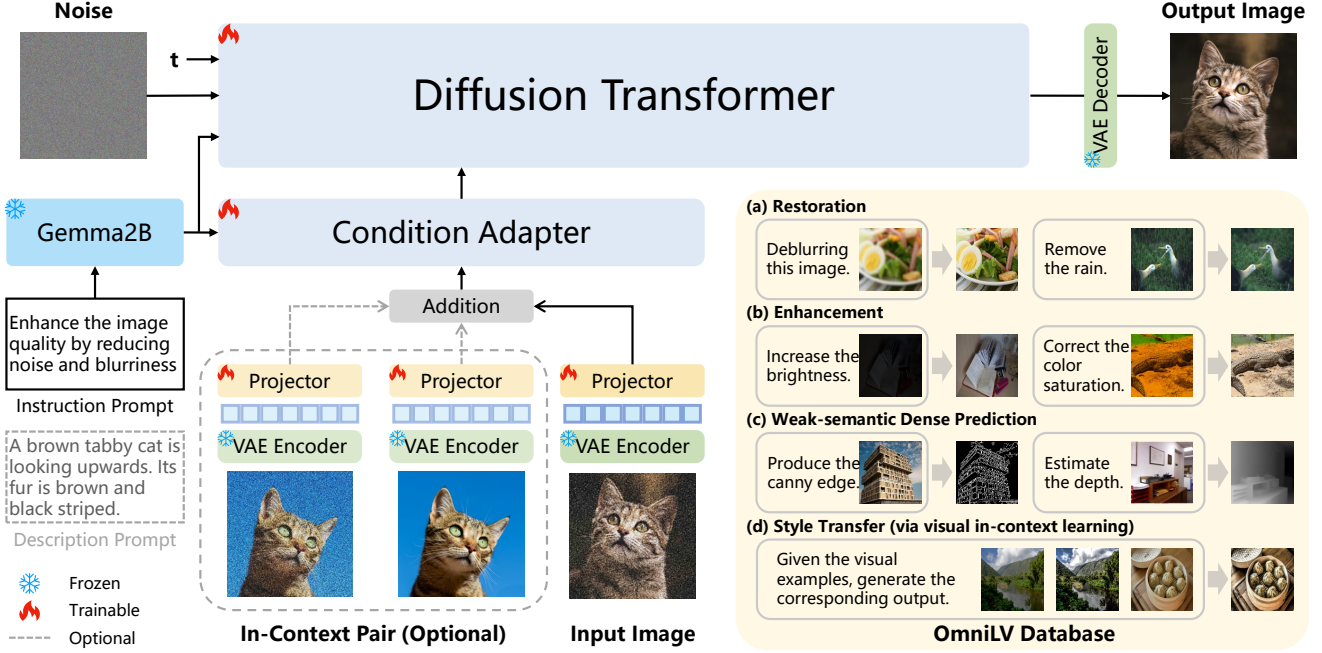


Figure 5. **Overall framework of OmniLV.** First, input images are encoded into latent space by VAE encoder. Then, we patchify the image latent and noise latent into visual tokens. Optionally, in-context pairs can be added to visual tokens to handle complex scenarios. At the same time, the instruction prompt and description prompt are processed by Gemma2B. Finally, we decode the denoised results to get the desired output images.

	Compression		Quantization		Noise		Inpainting	
	PSNR↑	MUSIQ↑	PSNR↑	MUSIQ↑	PSNR↑	MUSIQ↑	PSNR↑	MUSIQ↑
Addition	21.92	56.31	18.72	55.71	22.34	59.31	19.94	56.96
Concat	21.93	55.99	18.18	55.11	22.35	57.13	19.86	55.95

Table 2. Ablation study on whether to use addition or concatenation in in-context learning scenarios.

3.1.4. Enabling In-Context Learning

While text prompts can effectively guide tasks, many low-level vision tasks (e.g., stylization) require precise visual instructions that are difficult to express linguistically. To address this, we compare two paradigms for visual prompt integration: (1) **Input Concatenation** [24, 96, 98], where visual prompts are concatenated along the token dimension:

$$\mathbf{H}_{\text{fused}} = [\mathbf{H}_{\text{img}}; \mathbf{H}_{\text{prompt}_1}; \dots; \mathbf{H}_{\text{prompt}_n}], \quad (1)$$

where \mathbf{H}_{img} and $\mathbf{H}_{\text{prompt}_i}$ denote latent representation of input image and latent representation of i -th visual prompt, and $\mathbf{H}_{\text{fused}}$ denotes the combined latent representation. (2) **Projection-Addition** [95], which employs lightweight projectors to align visual prompts with the latent space before summation:

$$\mathbf{H}_{\text{fused}} = \mathbf{H}_{\text{image}} + \sum_{i=1}^n \phi_i(\mathbf{H}_{\text{prompt}_i}), \quad (2)$$

where $\phi(\cdot)$ denotes linear projectors. Fig. 5 illustrates the architectural differences between these two approaches, where the concatenation method can be seen as a variation where the ‘‘Projector-Addition’’ module is replaced with a Concatenation operation. Tab. 2 presents the quantitative comparison, demonstrating that projection-addition outperforms input concatenation across different tasks. This suggests that projection-based alignment better preserves task-relevant information.

Final Architecture. Based on these insights, we design the final architecture of OmniLV, as illustrated in Fig. 5. Our approach unifies diverse low-level vision tasks while ensuring strong multimodal conditioning and in-context learning capabilities.

3.2. Large-Scale OmniLV Dataset

To build a universal low-level vision model, we construct a large-scale multi-task dataset containing 40 million instances over 100 sub-tasks across four major domains: image restoration, image enhancement, dense prediction, and stylization. The main categories and distribution of OmniLV dataset are illustrated in Fig. 6. The dataset is sourced from publicly available collections and synthetically generated pairs, with additional high-quality data created through internal pipelines.

Image Restoration. The restoration dataset covers 23 major tasks with a total of 45 sub-tasks, addressing various

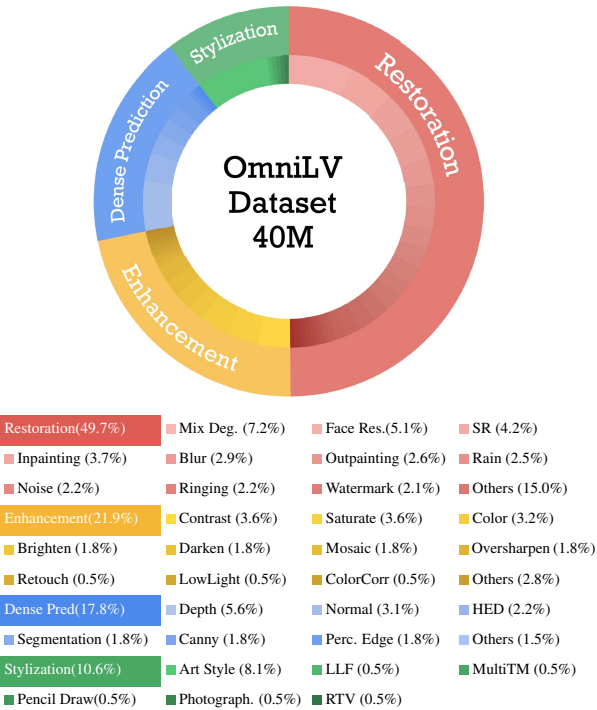


Figure 6. OmniLV dataset distribution with main categories.

degradation types such as motion blur, noise, and weather-induced distortions. It consists of both real-world degraded images and synthetic degradation pairs, carefully processed alongside high-quality ground truth images to ensure realism and diversity.

Image Enhancement. The enhancement dataset includes 14 major tasks with a total of 25 sub-tasks, covering tasks such as low-light correction, contrast enhancement, and saturation refinement. The dataset is composed of professionally edited reference images alongside algorithmically generated enhancement pairs, ensuring controlled transformations that align with perceptual quality.

Weak-semantic Dense Prediction. For dense prediction tasks, we compile annotated datasets for 10 tasks, including edge detection, depth estimation, and surface normal prediction. Each sample contains pixel-level ground truth annotations paired with descriptive task-specific instructions, facilitating multimodal learning.

Image Stylization. The stylization dataset spans 20 tasks, covering artistic transformations across various styles and techniques. It includes both real-world artistic works and style-transferred images generated by neural algorithms, ensuring a diverse range of stylish effects. We implement in-context learning on image stylization tasks due to the difficulty of defining task prompt.

Dataset Summary and Test Set Construction. In total, OmniLV dataset comprises four major task categories with over 100 sub-tasks and approximately 40 million training instances. For publicly available datasets, we directly adopt

their corresponding test sets for evaluation. For our synthesized tasks, we construct test sets based on DIV2K-val, forming OmniLV-Test (OLV-T). The OLV-T test set consists of 44 task-specific test sets, each containing 100 images, resulting in a total of 4,400 test images with 1k resolution. Further details on dataset partitioning and evaluation can be found in the Supplementary.

3.3. Model Training and Sampling Settings

The training of OmniLV is divided into three stages: In the first stage, we train the model with images at a resolution of 512^2 , focusing solely on single-image tasks. We use a constant learning rate of 1e-4 and train for 100k steps with a batch size of 512. The second stage adds in-context learning (ICL) tasks. We continue training for another 100k steps, maintaining the same learning rate of 1e-4 and batch size of 512. Finally, in the third stage, we increase the resolution to 1024^2 and train on all tasks. The batch size is reduced to 128, and the learning rate remains at 1e-4. This final stage ensures that the model is trained to handle a variety of tasks and image sizes effectively. The model is trained using 16 A100 GPUs.

4. Experiments

4.1. Comparisons with Existing Works

As a universal model, OmniLV exhibits superior abilities for various low-level vision tasks, even compared with existing task-specific models. We compare our method with task-specific methods [15, 22, 58, 87, 92, 101, 109, 110, 115], all-in-one methods [22, 45, 69], visual prompt methods [23, 63, 93], and text-guided diffusion methods [57, 107]. Some of them are constrained to generating images of fixed size. In our comparison, we resize the generated image to target image size to facilitate fair comparisons. We conduct comparisons on both synthetic and real-world data. We selected full-reference metric PSNR and non-reference metric MUSIQ [47] for quantitative comparison.

Image Restoration. Tab. 3 demonstrates that OmniLV achieves the highest PSNR scores across all restoration benchmarks when compared with diffusion-based models. We demonstrate the qualitative comparisons in Fig. 7 on general low-level tasks. In addition, the MUSIQ scores of OmniLV are highly competitive on most benchmarks, further underscoring its strong performance. Notably, on the Blind Image Restoration (BIR) and Face benchmarks, OmniLV, as a universal model, attains performance levels that are comparable to those of state-of-the-art specialized models, thereby validating its effectiveness in handling diverse restoration tasks.

Image Enhancement. As reported in Tab. 4, OmniLV significantly improves upon existing enhancement methods. The improvements highlight OmniLV’s ability to effectively enhance image quality while maintaining natural

Category	Method	Deblur		Compression		Denoise		Derain		Desnow		BIR	Face
		OLV-T(6 types)	RealBlurJ [82]	OLV-T(2 types)	OLV-T(6 types)	SIDD [2]	Synthetic	Rain1400 [33]	Snow100K-L [65]	DIV2K [6]	CelebA [66]		
Specialized	X-Restormer [22]	21.18/45.17	26.57/50.41	—	27.19 /63.67	31.95/22.04	27.10/71.34	32.35/70.34	—	—	—	—	—
	MPRNnet [110]	20.33/43.35	26.51/48.45	—	24.53/45.66	39.63/22.34	25.16/69.40	32.04/69.98	—	—	—	—	—
	MAXIM [87]	21.39/44.13	29.99 /55.68	—	24.75/49.30	39.68 /22.39	25.82/71.15	32.25/70.27	—	—	—	—	—
	DiffBIR [58]	—	—	—	—	—	—	—	—	—	—	22.77 /67.01	—
	GFPGAN [92]	—	—	—	—	—	—	—	—	—	—	25.80 /69.76	—
All-in-One Restoration	CodeFormer [115]	—	—	—	—	—	—	—	—	—	—	—	25.15 / 75.55
	X-Restormer [22]	21.44/39.73	26.23 /38.84	—	25.96 / 62.42	24.06/20.84	23.28 / 69.00	32.12 / 70.26	—	—	—	—	—
	DA-CLIP [69]	19.94/34.98	18.82/39.22	—	22.99/44.89	26.40/29.25	23.15/53.18	26.44/67.78	—	—	—	—	—
Visual-Prompt-based	AutoDIR [45]	20.09/45.07	19.10/ 49.63	—	26.46 /57.80	22.19/28.72	25.33 /64.59	26.21 / 70.75	—	—	—	—	—
	Painter [93]	17.05/28.74	15.37/28.79	17.84/34.43	18.04/37.11	38.65 /21.57	17.84/34.43	27.92/62.38	20.30/47.60	—	—	—	—
	PromptGIP [63]	20.01/31.26	22.94/29.65	21.93/35.15	22.80/35.58	26.16/22.79	21.93/35.15	23.87/50.62	20.29/40.21	—	—	—	—
Text-Prompt-based	GenLV [23]	22.15 /33.00	25.53/29.12	23.59 /35.96	23.51/38.21	30.41/ 28.10	23.59/35.96	26.26/56.99	20.21/45.61	—	—	—	—
	PromptFix [107]	20.32/43.75	26.14/39.37	18.10/50.41	14.59/51.77	24.25/21.22	18.10/50.41	21.61/63.07	21.12 /53.83	13.77/29.49	—	—	—
	PixWizard [57]	17.90/ 64.19	23.34/ 55.97	18.99/ 62.40	17.22/63.05	27.60/ 23.63	18.99/62.40	23.84/66.89	21.12 / 61.41	19.03 / 59.90	—	—	—
Multi-Modal Instruction	OmniLV	22.57 / 68.95	28.24 /36.09	22.93 / 68.99	23.53/ 69.23	32.96 /22.42	22.93/ 68.99	24.98/65.66	24.57 / 61.19	22.36 / 69.55	25.04 / 70.70	—	—

Table 3. Quantitative comparison on restoration tasks. **Red** and **blue** colors represent the best and second best performance, respectively, excluding specialized models. All values are reported as PSNR↑/MUSIQ↑. For specialized models, if a model achieves the best value, the corresponding number is highlighted in **bold**.

Category	Method	Brighten		Darken		Low light		Photoretouching		Contrast Adjust		Saturation Adjust	Oversharpening
		OLV-T(4 types)	OLV-T(4 types)	OLV-T(4 types)	OLV-T(4 types)	LOLV2-Real [103]	MIT5K [14]	OLV-T(4 types)	OLV-T(4 types)	OLV-T(4 types)	OLV-T(4 types)	OLV-T(1 type)	OLV-T(1 type)
Specialized	Retinexformer [15]	—	16.72/65.73	22.79/59.30	16.12/63.24	—	—	—	—	—	—	—	—
	MIRNet [109]	—	16.35/65.45	28.10/63.35	19.37 / 65.59	—	—	—	—	—	—	—	—
	MAXIM [87]	—	16.09/67.16	34.04 / 70.75	14.98/62.90	—	—	—	—	—	—	—	—
All-in-One Restoration	DA-CLIP [69]	—	14.91/53.04	26.64/ 67.73	—	—	—	—	—	—	—	—	—
	AutoDIR [45]	—	15.48/64.74	24.16/ 67.91	—	—	—	—	—	—	—	—	—
Visual-Prompt-based	Painter [93]	12.00/36.77	13.96/37.09	29.44 /53.82	17.19/58.39	12.55/35.99	13.25/36.66	—	—	—	—	—	—
	PromptGIP [63]	15.46/35.43	17.85/33.89	21.35 /38.18	16.57/43.02	15.80/33.75	16.63/34.49	16.63/38.74	—	—	—	—	—
	GenLV [23]	21.11 /40.16	21.70 /39.31	21.01/50.84	24.91 / 56.08	21.58 /39.46	20.87 /40.29	21.69 /37.08	—	—	—	—	—
Text-Prompt-based	PromptFix [107]	10.55/57.78	10.15/54.40	17.16/63.54	11.09/52.89	11.34/57.76	12.31/58.49	14.93/56.01	—	—	—	—	—
	PixWizard [57]	11.16/ 64.14	13.81/ 65.44	14.07/62.11	15.99/ 63.59	13.12/ 65.51	12.77/ 65.13	13.55/ 71.00	—	—	—	—	—
Multi-Modal Instruction	OmniLV	22.58 / 70.54	20.28 / 69.77	18.60/58.76	19.78 / 62.12	20.91 / 69.95	21.80 / 70.91	23.64 / 70.87	—	—	—	—	—

Table 4. Quantitative comparison on enhancement tasks.

details and color fidelity.

Dense Prediction. Tab. 5b presents the performance of various methods on dense prediction tasks, including depth estimation, normal estimation, and edge detection. Although OmniLV’s performance still lags behind that of specialized models, it demonstrates significant improvements over baseline methods, underscoring its potential as a universal framework for dense-prediction vision tasks.

Stylization. Tab. 5a illustrates that OmniLV also performs well on stylization tasks such as Local Laccian Filter (LLF) and Pencil Drawing [67]. Since stylization tasks are challenging to describe using natural language, we employed visual prompts to guide the model in processing images. OmniLV obtains balanced results in terms of objective quality and perceptual quality, thus validating its versatility across diverse low-level vision tasks.

4.2. More Exploration

Text Prompt vs. Visual Prompt. Our model supports both text prompt and visual prompt to guide the generation process. In Tab. 6, we present a detailed comparison between the two prompting methods across several low-level vision tasks, including deblurring, denoising, contrast adjustment,

and saturation adjustment. Adopting both prompts can yield better quality scores.

Relationship with High-Semantic Tasks. We further investigate the relationship between low-level vision tasks and high-semantic tasks such as image generation or image editing tasks [12, 40, 84, 85, 105, 112, 114]. As shown in Tab. 7, when high-semantic tasks are included in the training data, the performance on low-level vision tasks degrades. Specifically, performance for various tasks is consistently lower when high-semantic tasks are incorporated. This degradation arises because high-semantic tasks prioritize conceptual coherence and structural abstraction over pixel-accurate reconstruction, which conflicts with the objectives of low-level vision tasks that demand fine-grained texture recovery and precise detail preservation.

Generalization Exploration. We investigated the generalizability of OmniLV in terms of domain-specific adaptation and real-world robustness. Specifically, we selected images with various real-world degradations to comprehensively assess the model’s performance. As shown in Fig. 8, OmniLV effectively restores images in these diverse conditions, demonstrating its robustness and versatility in han-

Category	Method	LLF		PencilDrawing		Method	Depth Esti.		Normal Esti.		Method	HED	
		PSNR↑	FID↓	PSNR↑	FID↓		RMSE↓	Method	Mean Angle Error↓	Method		MAE↓	
Visual-Prompt-based	Painter [93]	13.64	120.3	8.434	157.5	–	–	–	–	PromptGIP	127.41		
	PromptGIP [63]	22.87	50.61	21.35	132.5	D.A.[101]	0.291	InvPT[104]	19.04	GenLV	94.68		
	GenLV [23]	25.66	29.53	28.29	38.70	Pixwizard [57]	0.941	Pixwizard	19.65	Pixwizard	103.45		
Multi-Modal Instruction	OmniLV	21.72	24.16	20.33	54.18	OmniLV	0.525	OmniLV	17.30	OmniLV	89.17		

(a) Stylization Tasks.

(b) Dense Prediction Tasks.

Table 5. Quantitative comparison on stylization tasks and weak-semantic dense prediction tasks.



Figure 7. Comparison results for low-level vision tasks. More results can be found in the Supplementary.

Text	Visual	Blur		Noise		Contrast Adju.		Saturate Adju.	
		PSNR↑	MUSIQ↑	PSNR↑	MUSIQ↑	PSNR↑	MUSIQ↑	PSNR↑	MUSIQ↑
✓	✗	22.57	68.95	23.53	69.23	20.90	69.95	21.79	70.90
✗	✓	21.99	67.59	22.71	67.66	20.09	66.58	20.14	68.08
✓	✓	22.50	68.99	23.07	69.37	20.50	70.09	21.00	70.91

Table 6. Effects of Various Prompt Formats. Our approach supports text prompts, visual prompts, or a combination of both.

High-semantic?	Blur		Noise		Contrast Adju.		Saturate Adju.	
	PSNR↑	MUSIQ↑	PSNR↑	MUSIQ↑	PSNR↑	MUSIQ↑	PSNR↑	MUSIQ↑
✗	21.13	58.78	22.34	57.39	19.03	56.95	18.64	56.60
✓	20.97	57.06	22.18	59.31	18.76	55.80	18.58	56.55

Table 7. Ablation study for the training data.

dling complex real-world degradations, such as real-world restoration, deraining, desnowing, underwater image enhancement, and satellite image enhancement.

5. Conclusion

In this work, we introduce OmniLV, a unified multimodal framework for low-level vision that successfully handles over 100 sub-tasks, including image restoration, enhancement, weak-semantic dense prediction, and stylization. By leveraging both textual and visual prompts with generative

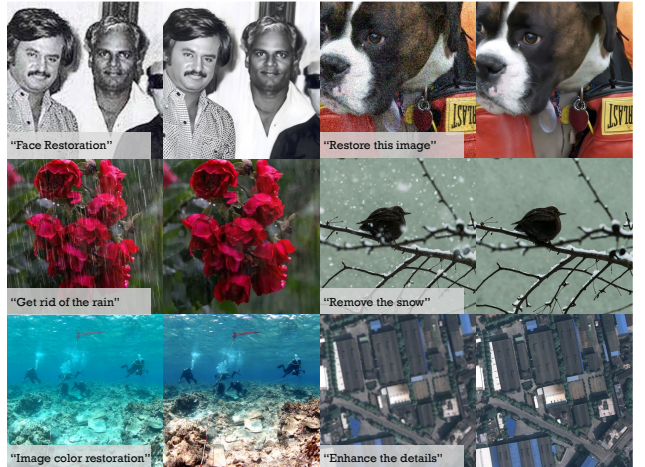


Figure 8. Examples of image restoration in various scenarios.

priors, OmniLV demonstrates robust generalization, high-

fidelity results, and flexibility across arbitrary resolutions. OmniLV achieves state-of-the-art performance in multiple low-level vision tasks and demonstrates promising generalization capabilities in real-world scenarios.

Limitations. Despite OmniLV’s extensive capability to handle a wide range of low-level vision tasks, it does not always achieve optimal performance in certain specialized scenarios. Future work will focus on improving task-specific performance through more refined model components and training strategies.

References

- [1] Andreas Aakerberg, Kamal Nasrollahi, and Thomas B Moeslund. Rellisur: A real low-light image super-resolution dataset. In *Thirty-fifth Conference on Neural Information Processing Systems-NeurIPS 2021*, 2021. [15](#)
- [2] Abdelrahman Abdelhamed, Stephen Lin, and Michael S Brown. A high-quality denoising dataset for smartphone cameras. In *Proceedings of the IEEE conference on computer vision and pattern recognition*, pages 1692–1700, 2018. [7, 15](#)
- [3] Josh Achiam, Steven Adler, Sandhini Agarwal, Lama Ahmad, Ilge Akkaya, Florencia Leoni Aleman, Diogo Almeida, Janko Altenschmidt, Sam Altman, Shyamal Anadkat, et al. Gpt-4 technical report. *arXiv preprint arXiv:2303.08774*, 2023. [2](#)
- [4] Mahmoud Afifi and Michael S Brown. Deep white-balance editing. In *Proceedings of the IEEE/CVF Conference on computer vision and pattern recognition*, pages 1397–1406, 2020. [15](#)
- [5] Mahmoud Afifi, Konstantinos G Derpanis, Bjorn Ommer, and Michael S Brown. Learning multi-scale photo exposure correction. In *Proceedings of the IEEE/CVF Conference on Computer Vision and Pattern Recognition*, pages 9157–9167, 2021. [15](#)
- [6] Eirikur Agustsson and Radu Timofte. Ntire 2017 challenge on single image super-resolution: Dataset and study. In *Proceedings of the IEEE conference on computer vision and pattern recognition workshops*, pages 126–135, 2017. [7, 15](#)
- [7] Yuang Ai, Xiaoqiang Zhou, Huaibo Huang, Xiaotian Han, Zhengyu Chen, Quanzeng You, and Hongxia Yang. Dream-clear: High-capacity real-world image restoration with privacy-safe dataset curation. In *The Thirty-eighth Annual Conference on Neural Information Processing Systems*, 2024. [3](#)
- [8] Jean-Baptiste Alayrac, Jeff Donahue, Pauline Luc, Antoine Miech, Iain Barr, Yana Hasson, Karel Lenc, Arthur Mensch, Katherine Millican, Malcolm Reynolds, et al. Flamingo: a visual language model for few-shot learning. *Advances in neural information processing systems*, 35: 23716–23736, 2022. [2](#)
- [9] Codruta O Ancuti, Cosmin Ancuti, Mateu Sbert, and Radu Timofte. Dense-haze: A benchmark for image dehazing with dense-haze and haze-free images. In *2019 IEEE international conference on image processing (ICIP)*, pages 1014–1018. IEEE, 2019. [15](#)
- [10] Codruta O Ancuti, Cosmin Ancuti, and Radu Timofte. Nh-haze: An image dehazing benchmark with non-homogeneous hazy and haze-free images. In *Proceedings of the IEEE/CVF conference on computer vision and pattern recognition workshops*, pages 444–445, 2020. [15](#)
- [11] Mathieu Aubry, Sylvain Paris, Samuel W Hasinoff, Jan Kautz, and Frédo Durand. Fast local laplacian filters: Theory and applications. *ACM Transactions on Graphics (TOG)*, 33(5):1–14, 2014. [15](#)
- [12] Tim Brooks, Aleksander Holynski, and Alexei A Efros. Instructpix2pix: Learning to follow image editing instructions. *arXiv preprint arXiv:2211.09800*, 2022. [7](#)
- [13] Vladimir Bychkovsky, Sylvain Paris, Eric Chan, and Frédo Durand. Learning photographic global tonal adjustment with a database of input / output image pairs. In *The Twenty-Fourth IEEE Conference on Computer Vision and Pattern Recognition*, 2011. [15](#)
- [14] Vladimir Bychkovsky, Sylvain Paris, Eric Chan, and Frédo Durand. Learning photographic global tonal adjustment with a database of input / output image pairs. In *The Twenty-Fourth IEEE Conference on Computer Vision and Pattern Recognition*, 2011. [7](#)
- [15] Yuanhao Cai, Hao Bian, Jing Lin, Haoqian Wang, Radu Timofte, and Yulun Zhang. Retinexformer: One-stage retinex-based transformer for low-light image enhancement. In *Proceedings of the IEEE/CVF international conference on computer vision*, pages 12504–12513, 2023. [2, 6, 7](#)
- [16] Bin Chen, Gehui Li, Rongyuan Wu, Xindong Zhang, Jie Chen, Jian Zhang, and Lei Zhang. Adversarial diffusion compression for real-world image super-resolution. *arXiv preprint arXiv:2411.13383*, 2024. [3](#)
- [17] Lin Chen, Jinsong Li, Xiaoyi Dong, Pan Zhang, Conghui He, Jiaqi Wang, Feng Zhao, and Dahua Lin. Sharegpt4v: Improving large multi-modal models with better captions. In *European Conference on Computer Vision*, pages 370–387. Springer, 2024. [14](#)
- [18] Wei-Ting Chen, Hao-Yu Fang, Cheng-Lin Hsieh, Cheng-Che Tsai, I Chen, Jian-Jiun Ding, Sy-Yen Kuo, et al. All snow removed: Single image desnowing algorithm using hierarchical dual-tree complex wavelet representation and contradict channel loss. In *Proceedings of the IEEE/CVF International Conference on Computer Vision*, pages 4196–4205, 2021. [15](#)
- [19] Xiangyu Chen, Yihao Liu, Zhengwen Zhang, Yu Qiao, and Chao Dong. Hdrunet: Single image hdr reconstruction with denoising and dequantization. In *Proceedings of the IEEE/CVF Conference on Computer Vision and Pattern Recognition*, pages 354–363, 2021. [2](#)
- [20] Xiangyu Chen, Zhengwen Zhang, Jimmy S Ren, Lynhoo Tian, Yu Qiao, and Chao Dong. A new journey from sdrtv to hdrtv. In *Proceedings of the IEEE/CVF International Conference on Computer Vision*, pages 4500–4509, 2021. [2](#)
- [21] Xiangyu Chen, Xintao Wang, Jiantao Zhou, Yu Qiao, and Chao Dong. Activating more pixels in image super-

resolution transformer. In *Proceedings of the IEEE/CVF conference on computer vision and pattern recognition*, pages 22367–22377, 2023. 2

[22] Xiangyu Chen, Zheyuan Li, Yuandong Pu, Yihao Liu, Jiantao Zhou, Yu Qiao, and Chao Dong. A comparative study of image restoration networks for general backbone network design. In *European Conference on Computer Vision*, pages 74–91. Springer, 2024. 2, 6, 7

[23] Xiangyu Chen, Yihao Liu, Yuandong Pu, Wenlong Zhang, Jiantao Zhou, Yu Qiao, and Chao Dong. Learning a low-level vision generalist via visual task prompt. In *Proceedings of the 32nd ACM International Conference on Multimedia*, pages 2671–2680, 2024. 2, 3, 6, 7, 8

[24] Xi Chen, Zhifei Zhang, He Zhang, Yuqian Zhou, Soo Ye Kim, Qing Liu, Yijun Li, Jianming Zhang, Nanxuan Zhao, Yilin Wang, et al. Unireal: Universal image generation and editing via learning real-world dynamics. *arXiv preprint arXiv:2412.07774*, 2024. 3, 5

[25] Zhe Chen, Weiyun Wang, Yue Cao, Yangzhou Liu, Zhangwei Gao, Erfei Cui, Jinguo Zhu, Shenglong Ye, Hao Tian, Zhaoyang Liu, et al. Expanding performance boundaries of open-source multimodal models with model, data, and test-time scaling. *arXiv preprint arXiv:2412.05271*, 2024. 2

[26] Zhe Chen, Weiyun Wang, Hao Tian, Shenglong Ye, Zhangwei Gao, Erfei Cui, Wenwen Tong, Kongzhi Hu, Jiapeng Luo, Zheng Ma, et al. How far are we to gpt-4v? closing the gap to commercial multimodal models with open-source suites. *Science China Information Sciences*, 67(12):220101, 2024.

[27] Zhe Chen, Jiannan Wu, Wenhui Wang, Weijie Su, Guo Chen, Sen Xing, Muyan Zhong, Qinglong Zhang, Xizhou Zhu, Lewei Lu, et al. Internvl: Scaling up vision foundation models and aligning for generic visual-linguistic tasks. In *Proceedings of the IEEE/CVF Conference on Computer Vision and Pattern Recognition*, pages 24185–24198, 2024. 2

[28] Yuekun Dai, Yihang Luo, Shangchen Zhou, Chongyi Li, and Chen Change Loy. Nighttime smartphone reflective flare removal using optical center symmetry prior. In *Proceedings of the IEEE Conference on Computer Vision and Pattern Recognition (CVPR)*, 2023. 15

[29] Chao Dong, Chen Change Loy, Kaiming He, and Xiaou Tang. Image super-resolution using deep convolutional networks. *IEEE transactions on pattern analysis and machine intelligence*, 38(2):295–307, 2015. 2

[30] Zheng Dong, Ke Xu, Yin Yang, Hujun Bao, Weiwei Xu, and Rynson W.H. Lau. Location-aware single image reflection removal. *ArXiv*, abs/2012.07131, 2020. 15

[31] Zheng Dong, Ke Xu, Yin Yang, Hujun Bao, Weiwei Xu, and Rynson WH Lau. Location-aware single image reflection removal. In *Proceedings of the IEEE/CVF international conference on computer vision*, pages 5017–5026, 2021. 15

[32] Patrick Esser, Sumith Kulal, Andreas Blattmann, Rahim Entezari, Jonas Müller, Harry Saini, Yam Levi, Dominik Lorenz, Axel Sauer, Frederic Boesel, et al. Scaling rectified flow transformers for high-resolution image synthesis. In *Forty-first international conference on machine learning*, 2024. 2, 3

[33] Xueyang Fu, Jiabin Huang, Delu Zeng, Yue Huang, Xinghao Ding, and John Paisley. Removing rain from single images via a deep detail network. In *Proceedings of the IEEE conference on computer vision and pattern recognition*, pages 3855–3863, 2017. 7

[34] Peng Gao, Le Zhuo, Chris Liu, Ruoyi Du, Xu Luo, Longtian Qiu, Yuhang Zhang, et al. Lumina-t2x: Transforming text into any modality, resolution, and duration via flow-based large diffusion transformers. *arXiv preprint arXiv:2405.05945*, 2024. 3

[35] Leon A Gatys, Alexander S Ecker, and Matthias Bethge. Image style transfer using convolutional neural networks. In *Proceedings of the IEEE conference on computer vision and pattern recognition*, pages 2414–2423, 2016. 2

[36] Yu Guo, Yuan Gao, Yuxu Lu, Ryan Wen Liu, and Shengfeng He. Onerestore: A universal restoration framework for composite degradation. In *European Conference on Computer Vision*, 2024. 2

[37] Zhen Han, Zeyinzi Jiang, Yulin Pan, Jingfeng Zhang, Chaojie Mao, Chenwei Xie, Yu Liu, and Jingren Zhou. Ace: All-round creator and editor following instructions via diffusion transformer. *arXiv preprint arXiv:2410.00086*, 2024. 3

[38] Jonathan Ho, Ajay Jain, and Pieter Abbeel. Denoising diffusion probabilistic models. *Advances in neural information processing systems*, 33:6840–6851, 2020. 2, 3

[39] Xun Huang and Serge Belongie. Arbitrary style transfer in real-time with adaptive instance normalization. In *Proceedings of the IEEE international conference on computer vision*, pages 1501–1510, 2017. 2

[40] Mude Hui, Siwei Yang, Bingchen Zhao, Yichun Shi, Heng Wang, Peng Wang, Yuyin Zhou, and Cihang Xie. Hq-edit: A high-quality dataset for instruction-based image editing. *arXiv preprint arXiv:2404.09990*, 2024. 7

[41] Andrey Ignatov, Jagruti Patel, and Radu Timofte. Rendering natural camera bokeh effect with deep learning. In *Proceedings of the IEEE/CVF Conference on Computer Vision and Pattern Recognition Workshops*, pages 418–419, 2020. 15

[42] Andrey Ignatov, Luc Van Gool, and Radu Timofte. Replacing mobile camera isp with a single deep learning model. In *Proceedings of the IEEE/CVF conference on computer vision and pattern recognition workshops*, pages 536–537, 2020. 15

[43] Huaizu Jiang, Jingdong Wang, Zejian Yuan, Yang Wu, Nanning Zheng, and Shipeng Li. Salient object detection: A discriminative regional feature integration approach. In *Proceedings of the IEEE conference on computer vision and pattern recognition*, pages 2083–2090, 2013. 15

[44] Kui Jiang, Zhongyuan Wang, Peng Yi, Chen Chen, Baojin Huang, Yimin Luo, Jiayi Ma, and Junjun Jiang. Multi-scale progressive fusion network for single image deraining. In *IEEE/CVF Conference on Computer Vision and Pattern Recognition (CVPR)*, 2020. 15

[45] Yitong Jiang, Zhaoyang Zhang, Tianfan Xue, and Jinwei Gu. Autodir: Automatic all-in-one image restoration with

latent diffusion. *arXiv preprint arXiv:2310.10123*, 2023. 6, 7

[46] Tero Karras, Samuli Laine, and Timo Aila. A style-based generator architecture for generative adversarial networks. In *Proceedings of the IEEE/CVF conference on computer vision and pattern recognition*, pages 4401–4410, 2019. 15

[47] Junjie Ke, Qifei Wang, Yilin Wang, Peyman Milanfar, and Feng Yang. Musiq: Multi-scale image quality transformer. In *Proceedings of the IEEE/CVF international conference on computer vision*, pages 5148–5157, 2021. 6

[48] Alexander Kirillov, Eric Mintun, Nikhila Ravi, Hanzi Mao, Chloe Rolland, Laura Gustafson, Tete Xiao, Spencer Whitehead, Alexander C Berg, Wan-Yen Lo, et al. Segment anything. In *Proceedings of the IEEE/CVF international conference on computer vision*, pages 4015–4026, 2023. 2

[49] Black Forest Labs. Flux. <https://github.com/black-forest-labs/flux>, 2024. 3

[50] Duong H. Le, Tuan Pham, Sangho Lee, Christopher Clark, Aniruddha Kembhavi, Stephan Mandt, Ranjay Krishna, and Jiasen Lu. One diffusion to generate them all, 2024. 3

[51] Duong H Le, Tuan Pham, Sangho Lee, Christopher Clark, Aniruddha Kembhavi, Stephan Mandt, Ranjay Krishna, and Jiasen Lu. One diffusion to generate them all. *arXiv preprint arXiv:2411.16318*, 2024. 2

[52] Boyi Li, Wenqi Ren, Dengpan Fu, Dacheng Tao, Dan Feng, Wenjun Zeng, and Zhangyang Wang. Benchmarking single-image dehazing and beyond. *IEEE Transactions on Image Processing*, 28(1):492–505, 2018. 15

[53] Boyun Li, Xiao Liu, Peng Hu, Zhongqin Wu, Jiancheng Lv, and Xi Peng. All-in-one image restoration for unknown corruption. In *Proceedings of the IEEE/CVF conference on computer vision and pattern recognition*, pages 17452–17462, 2022. 2

[54] Junnan Li, Dongxu Li, Caiming Xiong, and Steven Hoi. Blip: Bootstrapping language-image pre-training for unified vision-language understanding and generation. In *International conference on machine learning*, pages 12888–12900. PMLR, 2022. 14

[55] Ruoteng Li, Loong-Fah Cheong, and Robby T Tan. Heavy rain image restoration: Integrating physics model and conditional adversarial learning. In *Proceedings of the IEEE/CVF conference on computer vision and pattern recognition*, pages 1633–1642, 2019. 15

[56] Zhixin Liang, Chongyi Li, Shangchen Zhou, Ruicheng Feng, and Chen Change Loy. Iterative prompt learning for unsupervised backlit image enhancement. In *Proceedings of the IEEE/CVF International Conference on Computer Vision*, pages 8094–8103, 2023. 15

[57] Weifeng Lin, Xinyu Wei, Renrui Zhang, Le Zhuo, Shitian Zhao, Siyuan Huang, Huan Teng, Junlin Xie, Yu Qiao, Peng Gao, et al. Pixwizard: Versatile image-to-image visual assistant with open-language instructions. *arXiv preprint arXiv:2409.15278*, 2024. 3, 6, 7, 8

[58] Xinqi Lin, Jingwen He, Ziyan Chen, Zhaoyang Lyu, Bo Dai, Fanghua Yu, Yu Qiao, Wanli Ouyang, and Chao Dong. Diffbir: Toward blind image restoration with generative diffusion prior. In *European Conference on Computer Vision*, pages 430–448. Springer, 2024. 2, 3, 4, 6, 7

[59] Xingchao Liu, Chengyue Gong, and Qiang Liu. Flow straight and fast: Learning to generate and transfer data with rectified flow. *arXiv preprint arXiv:2209.03003*, 2022. 15

[60] Yihao Liu, Anran Liu, Jinjin Gu, Zhipeng Zhang, Wenhao Wu, Yu Qiao, and Chao Dong. Discovering distinctive” semantics” in super-resolution networks. *arXiv preprint arXiv:2108.00406*, 2021. 14

[61] Yang Liu, Zhen Zhu, and Xiang Bai. Wdnet: Watermark-decomposition network for visible watermark removal. In *2021 IEEE/CVF Winter Conference on Applications of Computer Vision (WACV)*. IEEE, 2021.

[62] Yang Liu, Zhen Zhu, and Xiang Bai. Wdnet: Watermark-decomposition network for visible watermark removal. In *Proceedings of the IEEE/CVF winter conference on applications of computer vision*, pages 3685–3693, 2021. 15

[63] Yihao Liu, Xiangyu Chen, Xianzheng Ma, Xintao Wang, Jiantao Zhou, Yu Qiao, and Chao Dong. Unifying image processing as visual prompting question answering. *arXiv preprint arXiv:2310.10513*, 2023. 2, 3, 6, 7, 8

[64] Yihao Liu, Hengyuan Zhao, Jinjin Gu, Yu Qiao, and Chao Dong. Evaluating the generalization ability of super-resolution networks. *IEEE Transactions on pattern analysis and machine intelligence*, 45(12):14497–14513, 2023. 14

[65] Yun-Fu Liu, Da-Wei Jaw, Shih-Chia Huang, and Jenq-Neng Hwang. Desnownet: Context-aware deep network for snow removal. *IEEE Transactions on Image Processing*, 27(6):3064–3073, 2018. 7, 15

[66] Ziwei Liu, Ping Luo, Xiaogang Wang, and Xiaoou Tang. Large-scale celebfaces attributes (celeba) dataset. *Retrieved August, 15(2018):11*, 2018. 7, 15

[67] Cewu Lu, Li Xu, and Jiaya Jia. Combining sketch and tone for pencil drawing production. In *Proceedings of the symposium on non-photorealistic animation and rendering*, pages 65–73, 2012. 7, 15

[68] Shenghong Luo, Xuhang Chen, Weiwen Chen, Zinuo Li, Shuqiang Wang, and Chi-Man Pun. Devignet: High-resolution vignetting removal via a dual aggregated fusion transformer with adaptive channel expansion. *Proceedings of the AAAI Conference on Artificial Intelligence*, 38(5):4000–4008, 2024. 15

[69] Ziwei Luo, Fredrik K Gustafsson, Zheng Zhao, Jens Sjölund, and Thomas B Schön. Controlling vision-language models for universal image restoration. *arXiv preprint arXiv:2310.01018*, 2023. 6, 7

[70] Chaojie Mao, Jingfeng Zhang, Yulin Pan, Zeyinzi Jiang, Zhen Han, Yu Liu, and Jingren Zhou. Ace++: Instruction-based image creation and editing via context-aware content filling. *arXiv preprint arXiv:2501.02487*, 2025. 3

[71] David Martin, Charless Fowlkes, Doron Tal, and Jitendra Malik. A database of human segmented natural images and its application to evaluating segmentation algorithms and measuring ecological statistics. In *Proceedings eighth IEEE international conference on computer vision. ICCV 2001*, pages 416–423. IEEE, 2001. 15

[72] Chong Mou, Xintao Wang, Liangbin Xie, Yanze Wu, Jian Zhang, Zhongang Qi, and Ying Shan. T2i-adapter: Learning adapters to dig out more controllable ability for text-to-image diffusion models. In *Proceedings of the AAAI Conference on Artificial Intelligence*, pages 4296–4304, 2024. 4

[73] Seungjun Nah, Tae Hyun Kim, and Kyoung Mu Lee. Deep multi-scale convolutional neural network for dynamic scene deblurring. In *Proceedings of the IEEE conference on computer vision and pattern recognition*, pages 3883–3891, 2017. 15

[74] William Peebles and Saining Xie. Scalable diffusion models with transformers. In *Proceedings of the IEEE/CVF international conference on computer vision*, pages 4195–4205, 2023. 2, 3

[75] Vaishnav Potlapalli, Syed Waqas Zamir, Salman Khan, and Fahad Khan. Promptir: Prompting for all-in-one image restoration. In *Thirty-seventh Conference on Neural Information Processing Systems*, 2023. 2

[76] Rui Qian, Robby T Tan, Wenhan Yang, Jiajun Su, and Jiaying Liu. Attentive generative adversarial network for raindrop removal from a single image. In *Proceedings of the IEEE conference on computer vision and pattern recognition*, pages 2482–2491, 2018. 15

[77] Liangqiong Qu, Jiandong Tian, Shengfeng He, Yandong Tang, and Rynson WH Lau. Deshadownet: A multi-context embedding deep network for shadow removal. In *Proceedings of the IEEE conference on computer vision and pattern recognition*, pages 4067–4075, 2017. 15

[78] Ruijie Quan, Xin Yu, Yuanzhi Liang, and Yi Yang. Removing raindrops and rain streaks in one go. In *Proceedings of the IEEE/CVF conference on computer vision and pattern recognition*, pages 9147–9156, 2021. 15

[79] René Ranftl, Katrin Lasinger, David Hafner, Konrad Schindler, and Vladlen Koltun. Towards robust monocular depth estimation: Mixing datasets for zero-shot cross-dataset transfer. *IEEE Transactions on Pattern Analysis and Machine Intelligence (TPAMI)*, 2020. 14

[80] Nikhila Ravi, Valentin Gabeur, Yuan-Ting Hu, Ronghang Hu, Chaitanya Ryali, Tengyu Ma, Haitham Khedr, Roman Rädle, Chloe Rolland, Laura Gustafson, et al. Sam 2: Segment anything in images and videos. *arXiv preprint arXiv:2408.00714*, 2024. 2

[81] Jaesung Rim, Haeyun Lee, Juchae Won, and Sunghyun Cho. Real-world blur dataset for learning and benchmarking deblurring algorithms. In *Computer vision–ECCV 2020: 16th European conference, glasgow, UK, August 23–28, 2020, proceedings, part XXV 16*, pages 184–201. Springer, 2020. 15

[82] Jaesung Rim, Haeyun Lee, Juchae Won, and Sunghyun Cho. Real-world blur dataset for learning and benchmarking deblurring algorithms. In *Proceedings of the European Conference on Computer Vision (ECCV)*, 2020. 7

[83] Robin Rombach, Andreas Blattmann, Dominik Lorenz, Patrick Esser, and Björn Ommer. High-resolution image synthesis with latent diffusion models. In *Proceedings of the IEEE/CVF conference on computer vision and pattern recognition*, pages 10684–10695, 2022. 2, 3

[84] Shelly Sheynin, Adam Polyak, Uriel Singer, Yuval Kirstain, Amit Zohar, Oron Ashual, Devi Parikh, and Yaniv Taigman. Emu edit: Precise image editing via recognition and generation tasks. In *Proceedings of the IEEE/CVF Conference on Computer Vision and Pattern Recognition*, pages 8871–8879, 2024. 7

[85] Jing Shi, Ning Xu, Trung Bui, Franck Dernoncourt, Zheng Wen, and Chenliang Xu. A benchmark and baseline for language-driven image editing. In *Proceedings of the Asian Conference on Computer Vision*, 2020. 7

[86] Nathan Silberman, Derek Hoiem, Pushmeet Kohli, and Rob Fergus. Indoor segmentation and support inference from rgbd images. In *Computer Vision – ECCV 2012*, pages 746–760, Berlin, Heidelberg, 2012. Springer Berlin Heidelberg. 14

[87] Zhengzhong Tu, Hossein Talebi, Han Zhang, Feng Yang, Peyman Milanfar, Alan Bovik, and Yinxiao Li. Maxim: Multi-axis mlp for image processing. *CVPR*, 2022. 6, 7

[88] Jianyi Wang, Zongsheng Yue, Shangchen Zhou, Kelvin CK Chan, and Chen Change Loy. Exploiting diffusion prior for real-world image super-resolution. *International Journal of Computer Vision*, 132(12):5929–5949, 2024. 3

[89] Longguang Wang, Yulan Guo, Yingqian Wang, Juncheng Li, Shuhang Gu, Radu Timofte, Ming Cheng, Haoyu Ma, Qiufang Ma, Xiaopeng Sun, et al. Ntire 2023 challenge on stereo image super-resolution: Methods and results. In *Proceedings of the IEEE/CVF conference on computer vision and pattern recognition*, pages 1346–1372, 2023. 15

[90] Ruixing Wang, Qing Zhang, Chi-Wing Fu, Xiaoyong Shen, Wei-Shi Zheng, and Jiaya Jia. Underexposed photo enhancement using deep illumination estimation. In *Proceedings of the IEEE/CVF conference on computer vision and pattern recognition*, pages 6849–6857, 2019. 2

[91] Weihan Wang, Qingsong Lv, Wenmeng Yu, Wenyi Hong, Ji Qi, Yan Wang, Junhui Ji, Zhuoyi Yang, Lei Zhao, Xixuan Song, Jiazheng Xu, Bin Xu, Juanzi Li, Yuxiao Dong, Ming Ding, and Jie Tang. Cogvlm: Visual expert for pretrained language models, 2023. 14

[92] Xintao Wang, Yu Li, Honglun Zhang, and Ying Shan. Towards real-world blind face restoration with generative facial prior. In *The IEEE Conference on Computer Vision and Pattern Recognition (CVPR)*, 2021. 6, 7

[93] Xinlong Wang, Wen Wang, Yue Cao, Chunhua Shen, and Tiejun Huang. Images speak in images: A generalist painter for in-context visual learning. *arXiv preprint arXiv:2212.02499*, 2022. 6, 7, 8

[94] Xinlong Wang, Xiaosong Zhang, Zhengxiong Luo, Quan Sun, Yufeng Cui, Jinsheng Wang, Fan Zhang, Yueze Wang, Zhen Li, Qiying Yu, et al. Emu3: Next-token prediction is all you need. *arXiv preprint arXiv:2409.18869*, 2024. 3

[95] Zhendong Wang, Yifan Jiang, Yadong Lu, Pengcheng He, Weizhu Chen, Zhangyang Wang, Mingyuan Zhou, et al. In-context learning unlocked for diffusion models. *Advances in Neural Information Processing Systems*, 36:8542–8562, 2023. 5

[96] Zhaoqing Wang, Xiaobo Xia, Runnan Chen, Dongdong Yu, Changhu Wang, Mingming Gong, and Tongliang Liu.

Lavin-dit: Large vision diffusion transformer. *arXiv preprint arXiv:2411.11505*, 2024. 5

[97] Rongyuan Wu, Lingchen Sun, Zhiyuan Ma, and Lei Zhang. One-step effective diffusion network for real-world image super-resolution. *Advances in Neural Information Processing Systems*, 37:92529–92553, 2024. 3

[98] Shitao Xiao, Yueze Wang, Junjie Zhou, Huaying Yuan, Xingrun Xing, Ruiran Yan, Shuting Wang, Tiejun Huang, and Zheng Liu. Omnigen: Unified image generation. *arXiv preprint arXiv:2409.11340*, 2024. 2, 3, 5

[99] Enze Xie, Junsong Chen, Junyu Chen, Han Cai, Haotian Tang, Yujun Lin, Zhekai Zhang, Muyang Li, Ligeng Zhu, Yao Lu, and Song Han. Sana: Efficient high-resolution image synthesis with linear diffusion transformer, 2024. 3

[100] Li Xu, Qiong Yan, Yang Xia, and Jiaya Jia. Structure extraction from texture via relative total variation. *ACM transactions on graphics (TOG)*, 31(6):1–10, 2012. 15

[101] Lihe Yang, Bingyi Kang, Zilong Huang, Xiaogang Xu, Jiashi Feng, and Hengshuang Zhao. Depth anything: Unleashing the power of large-scale unlabeled data. In *Proceedings of the IEEE/CVF Conference on Computer Vision and Pattern Recognition*, pages 10371–10381, 2024. 2, 6, 8

[102] Tao Yang, Rongyuan Wu, Peiran Ren, Xuansong Xie, and Lei Zhang. Pixel-aware stable diffusion for realistic image super-resolution and personalized stylization. In *European Conference on Computer Vision*, pages 74–91. Springer, 2024. 3

[103] Wenhao Yang, Shiqi Wang, Yuming Fang, Yue Wang, and Jiaying Liu. From fidelity to perceptual quality: A semi-supervised approach for low-light image enhancement. In *IEEE/CVF Conference on Computer Vision and Pattern Recognition (CVPR)*, 2020. 7, 15

[104] Hanrong Ye and Dan Xu. Inverted pyramid multi-task transformer for dense scene understanding. In *ECCV*, 2022. 8

[105] Ahmet Burak Yildirim, Vedat Baday, Erkut Erdem, Aykut Erdem, and Aysegul Dundar. Inst-inpaint: Instructing to remove objects with diffusion models, 2023. 7

[106] Fanghua Yu, Jinjin Gu, Zheyuan Li, Jinfan Hu, Xiangtao Kong, Xintao Wang, Jingwen He, Yu Qiao, and Chao Dong. Scaling up to excellence: Practicing model scaling for photo-realistic image restoration in the wild. In *Proceedings of the IEEE/CVF Conference on Computer Vision and Pattern Recognition*, pages 25669–25680, 2024. 2, 3, 4

[107] Yongsheng Yu, Ziyun Zeng, Hang Hua, Jianlong Fu, and Jiebo Luo. Promptfix: You prompt and we fix the photo. In *NeurIPS*, 2024. 6, 7

[108] Zongsheng Yue, Kang Liao, and Chen Change Loy. Arbitrary-steps image super-resolution via diffusion inversion. *arXiv preprint arXiv:2412.09013*, 2024. 3

[109] Syed Waqas Zamir, Aditya Arora, Salman Khan, Munawar Hayat, Fahad Shahbaz Khan, Ming-Hsuan Yang, and Ling Shao. Learning enriched features for real image restoration and enhancement. In *ECCV*, 2020. 2, 6, 7

[110] Syed Waqas Zamir, Aditya Arora, Salman Khan, Munawar Hayat, Fahad Shahbaz Khan, Ming-Hsuan Yang, and Ling Shao. Multi-stage progressive image restoration. In *CVPR*, 2021. 6, 7

[111] Kai Zhang, Wangmeng Zuo, Yunjin Chen, Deyu Meng, and Lei Zhang. Beyond a gaussian denoiser: Residual learning of deep cnn for image denoising. *IEEE transactions on image processing*, 26(7):3142–3155, 2017. 2

[112] Kai Zhang, Lingbo Mo, Wenhui Chen, Huan Sun, and Yu Su. Magicbrush: A manually annotated dataset for instruction-guided image editing. In *Advances in Neural Information Processing Systems*, 2023. 7

[113] Lvmin Zhang, Anyi Rao, and Maneesh Agrawala. Adding conditional control to text-to-image diffusion models. In *Proceedings of the IEEE/CVF International Conference on Computer Vision*, pages 3836–3847, 2023. 4

[114] Haozhe Zhao, Xiaojian Ma, Liang Chen, Shuzheng Si, Ruojie Wu, Kaikai An, Peiyu Yu, Minjia Zhang, Qing Li, and Baobao Chang. Ultraedit: Instruction-based fine-grained image editing at scale, 2024. 7

[115] Shangchen Zhou, Kelvin C.K. Chan, Chongyi Li, and Chen Change Loy. Towards robust blind face restoration with codebook lookup transformer. In *NeurIPS*, 2022. 6, 7

[116] Yurui Zhu, Tianyu Wang, Xueyang Fu, Xuanyu Yang, Xin Guo, Jifeng Dai, Yu Qiao, and Xiaowei Hu. Learning weather-general and weather-specific features for image restoration under multiple adverse weather conditions. In *Proceedings of the IEEE/CVF conference on computer vision and pattern recognition*, pages 21747–21758, 2023. 15

[117] Le Zhuo, Ruoyi Du, Xiao Han, Yangguang Li, Dongyang Liu, Rongjie Huang, Wenze Liu, et al. Lumina-next: Making lumina-t2x stronger and faster with next-dit. *arXiv preprint arXiv:2406.18583*, 2024. 3

A. Training Dataset

Our dataset comprises four major types of low-level vision tasks: image restoration, image enhancement, weak-semantic dense prediction, and stylization. The dataset is constructed from both open-source datasets and internal synthesized data. Fig. 9 is a detailed version of the dataset composition. For the synthesized portion, we generate corresponding low-quality (LQ) and high-quality (HQ) image pairs using various degradation algorithms combined with our internally curated high-quality images. For the description prompts associated with the synthesized data, we provide annotations of varying lengths using BLIP[54], CogVLM [91], and ShareGPT4V [17]. Additionally, we generate diverse task instructions for each task. In Fig. 12, we show examples of task prompts.

B. Evaluation Protocol

In our experiments, we use DIV2K-val as the source data and synthesize the corresponding test images with the same degradation algorithms applied in the training set. Since the output resolutions of the current baseline methods vary, we resize each output image to match the dimensions of the corresponding ground truth using Bicubic interpolation before computing evaluation metrics. PSNR and SSIM are calculated on the RGB color space. For depth estimation, we evaluate on the NYU-v2 test set [86], which only provides metric depth. However, similar to Depth Anything, OmniLV predicts relative depth maps (disparity). Therefore, following the approach in [79], we convert the predicted disparity into metric depth for a fair comparison.

C. Experiment Details

C.1. Structure of Condition Adapter

The condition adapter employs a 12 layer transformer with a linear layer to project condition features into DiT’s latent space.

C.2. Ablation Study Details

All ablation experiments are conducted under a consistent training configuration to ensure a fair comparison. Specifically, we adopt the first-stage training setup described in Section 3.3, using a resolution of 512^2 , 8 A100 GPUs, a batch size of 512, and a constant learning rate of 1e-4 for 100k training steps.

Multimodal Encoding Variants. To compare “separate versus unified” encoding strategies for integrating text instructions and visual exemplars, we use **Qwen-VL 2.5** as the unified multimodal encoder baseline. In the unified setting, both text and visual prompts are jointly encoded and passed to the diffusion model. In contrast, the separate encoding baseline decouples the two modalities, with text in-

structions processed by a language model and visual exemplars encoded via a visual VAE. Both variants are trained under identical conditions. The unified encoding model consistently underperforms due to modality interference, as discussed in the main paper and illustrated in Fig. 3. Following [60, 64], we perform t-SNE analysis on dense prediction tasks for 200 data points each.

Condition Integration Design. We investigate five different strategies for integrating condition features into the diffusion model:

- **ControlNet-style injection**, where the condition is processed by a parallel branch and injected into the main model without updating the backbone.
- **Input Concatenation** directly concatenates the condition image with the input of the target image, and jointly feeds them into the model.
- **First-half Addition**, where condition features are added to the latent representations in the early layers.
- **Second-half Addition**, where addition occurs only in the later layers of the model.
- **Interleaved Addition**, where condition features are added in alternating layers throughout the network.

All variants use the same condition adapter described in Section C.1. As shown in Table 1, early integration (first half) consistently yields better performance, suggesting that early-stage guidance plays a critical role in conditioning effectiveness.

In-Context Visual Prompting. We evaluate two visual prompt integration paradigms: (1) **Input Concatenation**, where prompt tokens are directly concatenated to the input token sequence; and (2) **Projection-Addition**, where each visual prompt is projected to the latent space and added to the input latent. Both settings use the same projector architecture and number of visual exemplars. As shown in Table 2, projection-addition performs better in most tasks, which we attribute to better alignment and reduced representation conflict in the fused latent space.

C.3. Training Loss

Specifically, let $(x, y) \sim q$ denote a pair of high-quality (hq) and low-quality (lq) images, respectively, and let $z \sim \mathcal{N}(0, I)$ be a noise sample. We define a target velocity field $u_t: [0, 1] \times \mathbb{R}^d \times \mathbb{R}^d \rightarrow \mathbb{R}^d$, which induces a flow $\phi_t: [0, 1] \times \mathbb{R}^d \times \mathbb{R}^d \rightarrow \mathbb{R}^d$, that continuously transforms the noise distribution into the high-quality image distribution conditioned on the low-quality input. This transformation is governed by the ordinary differential equation (ODE)

$$\frac{d}{dt} \phi_t(x | y) = u_t(\phi_t(x | y) | y), \quad (3)$$

with the initial condition $\phi_0(x | y) = x$.

In flow-based models, a neural network is trained to approximate the conditional expectation $\bar{u}_t = \mathbb{E}[u_t | x_t, y]$,

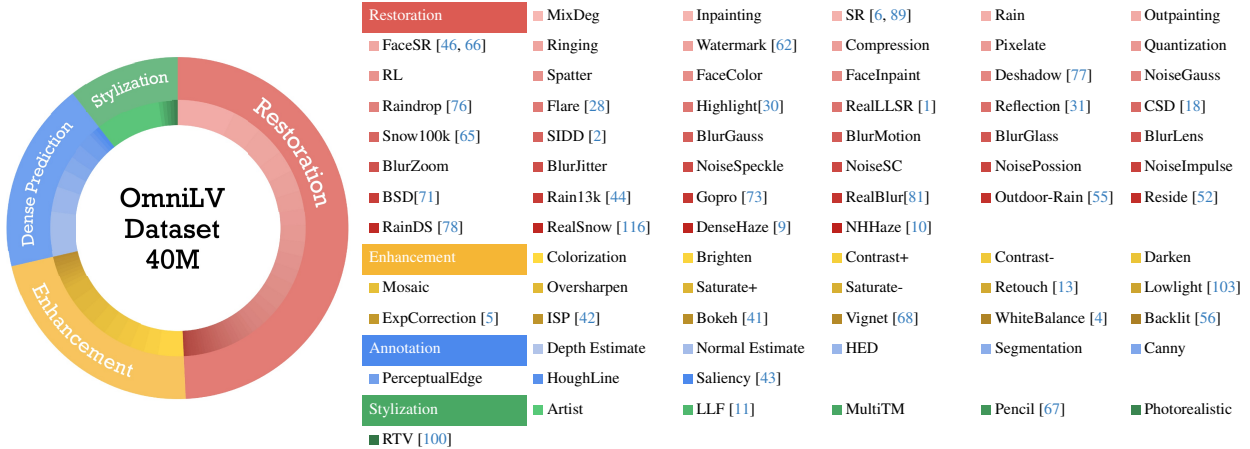


Figure 9. OmniLV dataset distribution with main categories.

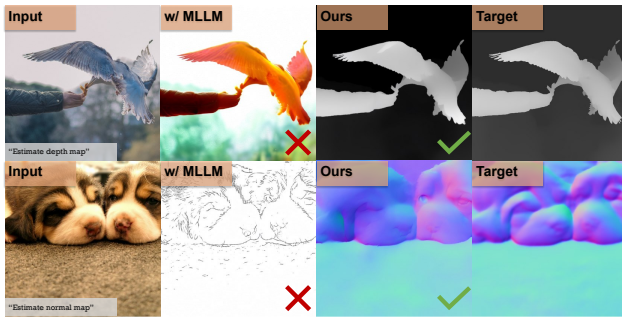


Figure 10. Task mismatch samples.

which represents an average over all plausible velocity fields at the state x_t given the conditioning variable y . Accordingly, we optimize our model using the conditional flow matching (CFM) objective as described in [59]

$$\mathcal{L}_{CFM}(\theta) = \mathbb{E}_{t, q(x_1, y), p_t(x|x_1)} \|u_\theta(t, x, y) - u_t(x|x_1)\| \quad (4)$$

where $t \sim \mathcal{U}[0, 1]$, x_1 and y are sampled from the data distribution, and $x \sim p_t(x|x_1)$.

D. More Results

Detailed Quantitative Results. In the main paper, we present quantitative results of several representative tasks. Here we provide a detailed quantitative results of more tasks, as summarized in Table 8, 9, 10, 11, 12, 13, and 14. This section provides more results for diverse tasks. Fig. 11 presents the results of OmniLV on colorization. Fig. 13 presents more results of dense prediction, including Canny edge detection, HED, relative depth estimation, and normal estimation. Fig. 14 presents results of stylization, mimicking local Laplacian filtering and pencil drawing. Fig. 15 and Fig. 16 present more results on image



Figure 11. More results of colorization.

enhancement, including retouching, saturation adjustment, contrast adjustment, and mosaic removal. Fig. 17, Fig. 18, Fig. 19, Fig. 20, Fig. 21, and Fig. 22 present more results on image restoration, including face restoration, deblurring, deraining, dehazing, denoising, JPEG compression artifact removal, mixed degradation restoration, inpainting, deshadowing, and dewatermark. It can be seen that OmniLV consistently follows the text or visual prompt to conduct the various low-level vision tasks, while other methods often fail to follow the instruction and yield bad results.

Blur 	Compression 	Raining 	Haze 
<ul style="list-style-type: none"> Sharpen this blurred image as described Remove the blur from this photo based on the following instructions Enhance the clarity of this blurry image according to these details 	<ul style="list-style-type: none"> Restore this compressed image according to the description Improve the quality of this compressed photo based on these instructions Enhance the details of the compressed picture as specified 	<ul style="list-style-type: none"> Remove the rain from this image based on the following description Clear the raindrops from the photo according to these instructions Eliminate the rainy effect in the picture as described below: 	<ul style="list-style-type: none"> Remove the haze from this image Clear the hazy effect from the photo Eliminate the haze in the picture
Inpainting 	Super Resolution 	Spatter 	Quantization 
<ul style="list-style-type: none"> Inpaint this image with the following description Fill in the missing parts of the image based on these instructions Restore the damaged areas of the picture as described below 	<ul style="list-style-type: none"> Enhance the resolution of this image Improve the image quality by increasing resolution Upscale the image resolution 	<ul style="list-style-type: none"> Remove the spatter from this image as described Clean up the spatter marks in the photo according to these instructions Eliminate the spatter effect from the picture based on the following 	<ul style="list-style-type: none"> Restore this quantized image according to the following details Improve the color depth of this quantized photo based on these instructions Enhance the color gradients in the quantized picture as specified
Brighten 	Darken 	Contrast 	Saturate 
<ul style="list-style-type: none"> Adjust the brightness of this image to a normal level Reduce the excessive brightness of the photo Lower the overall luminosity of the picture to a standard range as specified 	<ul style="list-style-type: none"> Lighten this image based on the following details Increase the brightness of the photo according to these instructions Raise the overall luminosity of the picture as specified 	<ul style="list-style-type: none"> Modify the contrast of this image to enhance details as described Tune the contrast settings of the image using this information Refine the contrast ratio in the photo to achieve a more natural appearance as per these guidelines: 	<ul style="list-style-type: none"> Adjust the saturation of this image as described Change the saturation levels in the picture based on the following Change the color saturation of the picture as instructed
Oversharpen 	Retouch 	Exposure 	BacklitEnhance 
<ul style="list-style-type: none"> Inpaint this image with the following description Fill in the missing parts of the image based on these instructions Restore the damaged areas of the picture as described below 	<ul style="list-style-type: none"> Enhance the resolution of this image Improve the image quality by increasing resolution Upscale the image resolution 	<ul style="list-style-type: none"> Remove the spatter from this image as described Clean up the spatter marks in the photo according to these instructions Eliminate the spatter effect from the picture based on the following 	<ul style="list-style-type: none"> Restore this quantized image according to the following details Improve the color depth of this quantized photo based on these instructions Enhance the color gradients in the quantized picture as specified
Canny Edge 	Normal Estimation 	Depth Estimation 	HED Edge 
<ul style="list-style-type: none"> Inpaint this image with the following description Fill in the missing parts of the image based on these instructions Restore the damaged areas of the picture as described below 	<ul style="list-style-type: none"> Enhance the resolution of this image Improve the image quality by increasing resolution Upscale the image resolution 	<ul style="list-style-type: none"> Remove the spatter from this image as described Clean up the spatter marks in the photo according to these instructions Eliminate the spatter effect from the picture based on the following 	<ul style="list-style-type: none"> Restore this quantized image according to the following details Improve the color depth of this quantized photo based on these instructions Enhance the color gradients in the quantized picture as specified

Figure 12. Examples of prompts for different tasks.

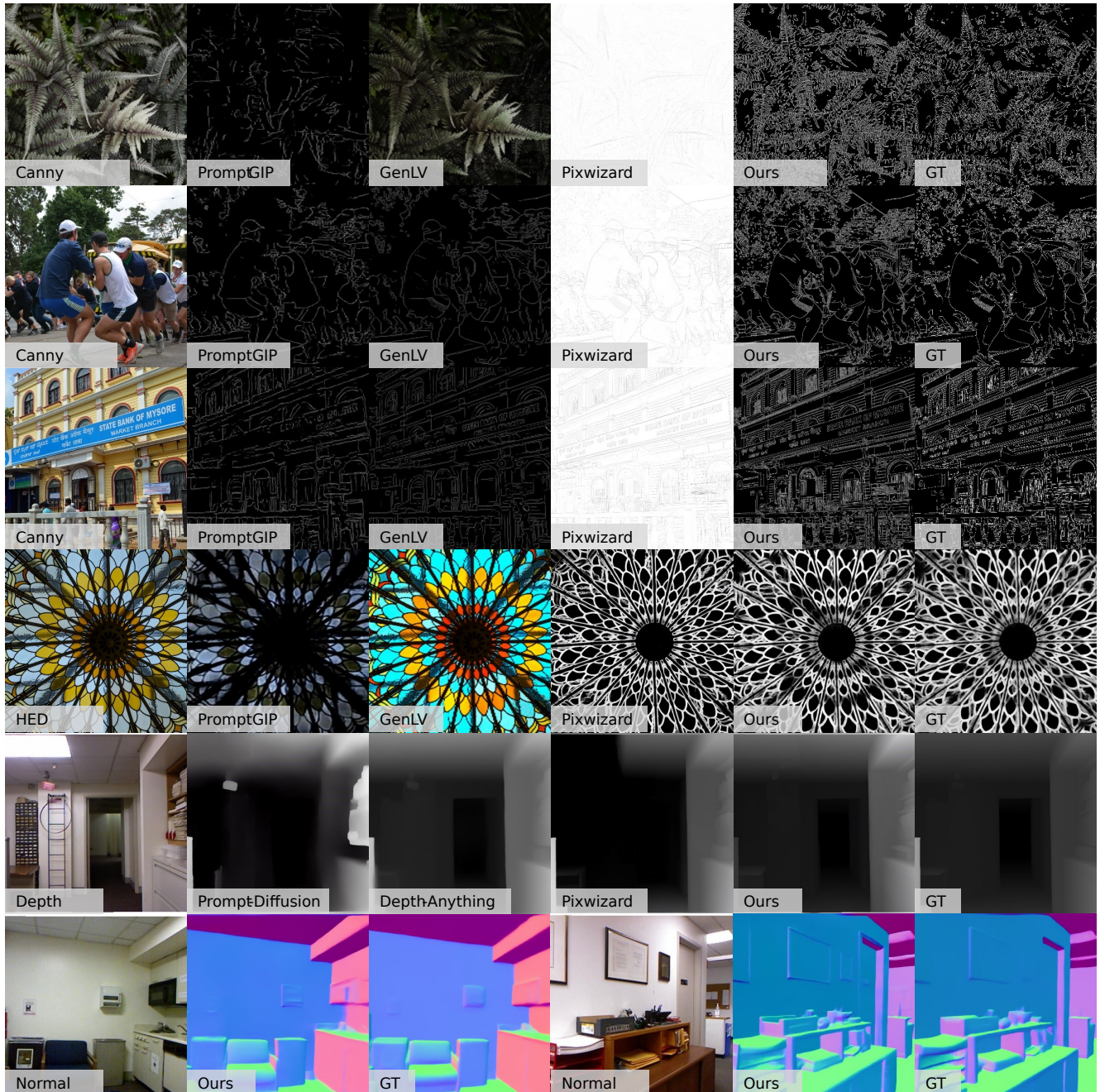


Figure 13. More results of dense prediction.



Figure 14. More results of stylization.

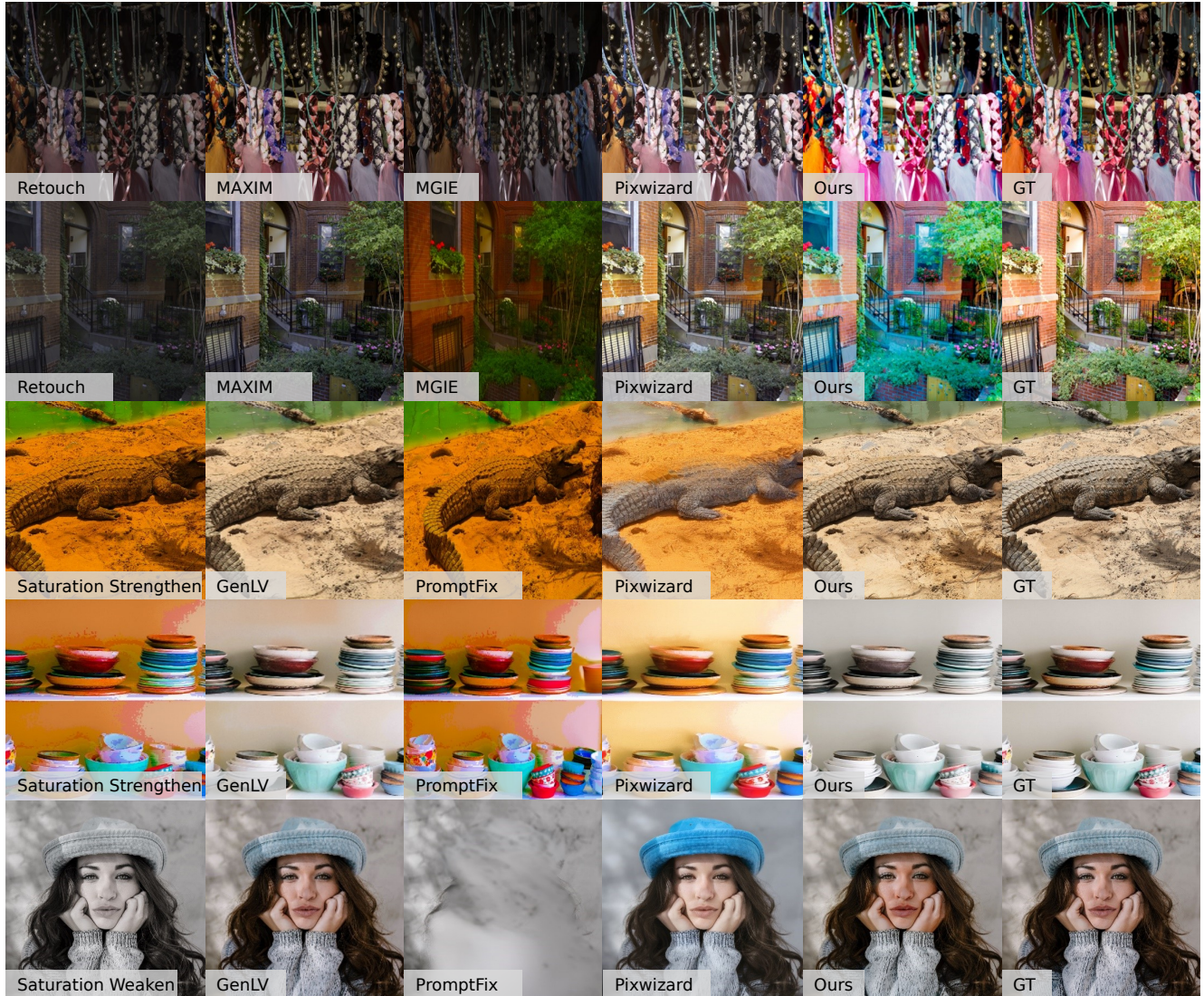


Figure 15. More results of image enhancement.

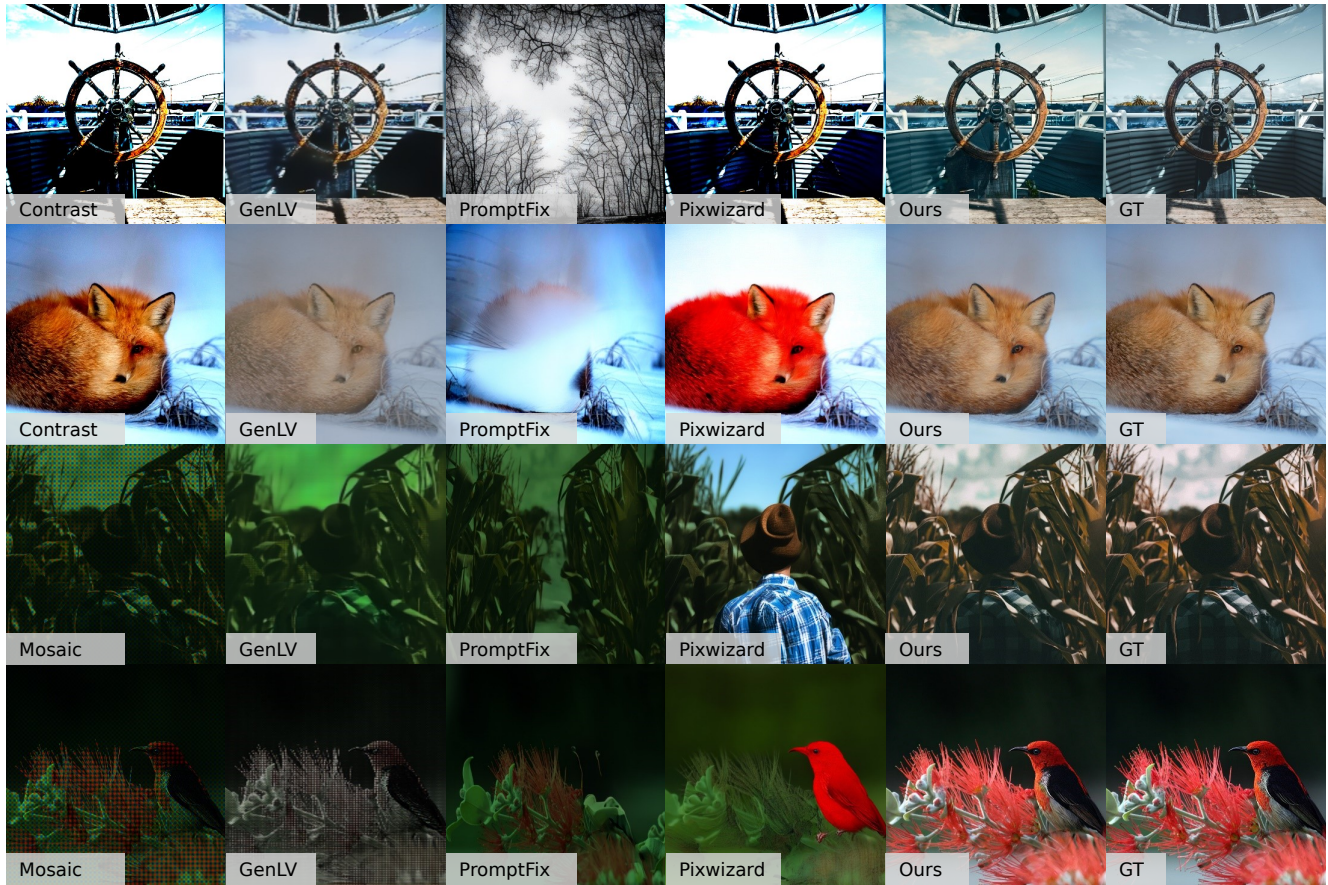


Figure 16. More results of image enhancement.



Figure 17. More results of face restoration.



Figure 18. More results of deblurring.

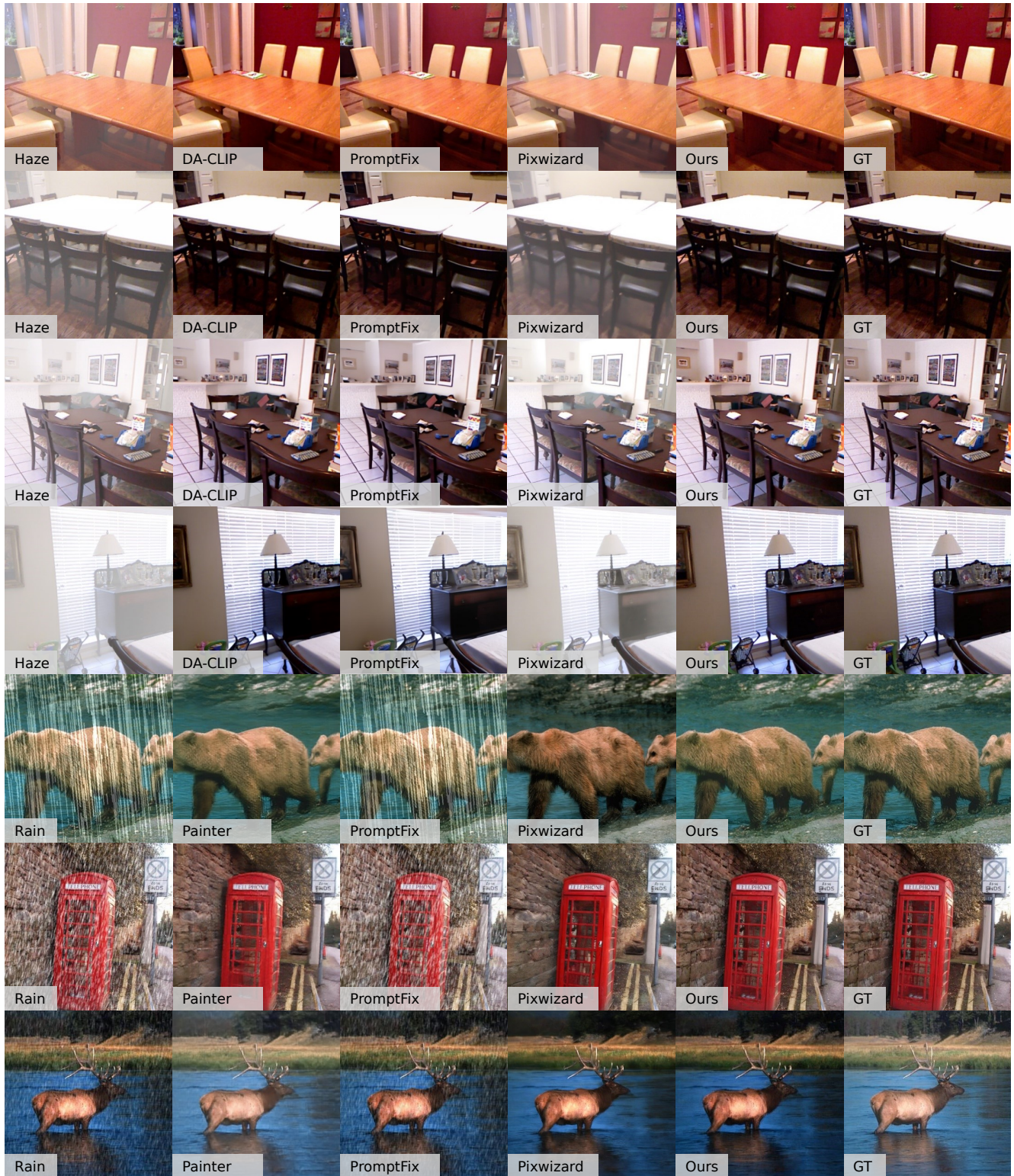


Figure 19. More results of dehazing and deraining.

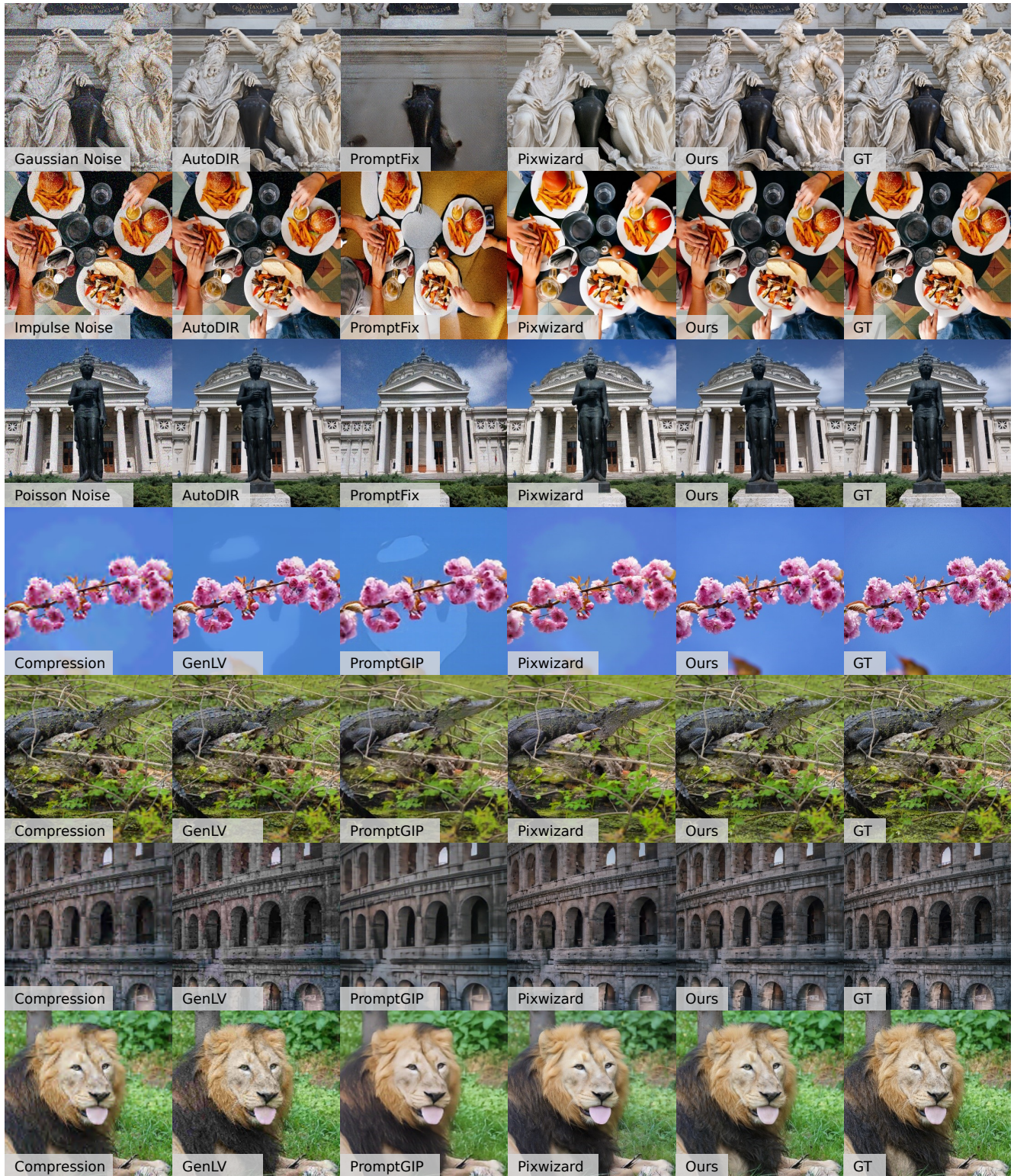


Figure 20. More results of denoising and compression artifact removal.

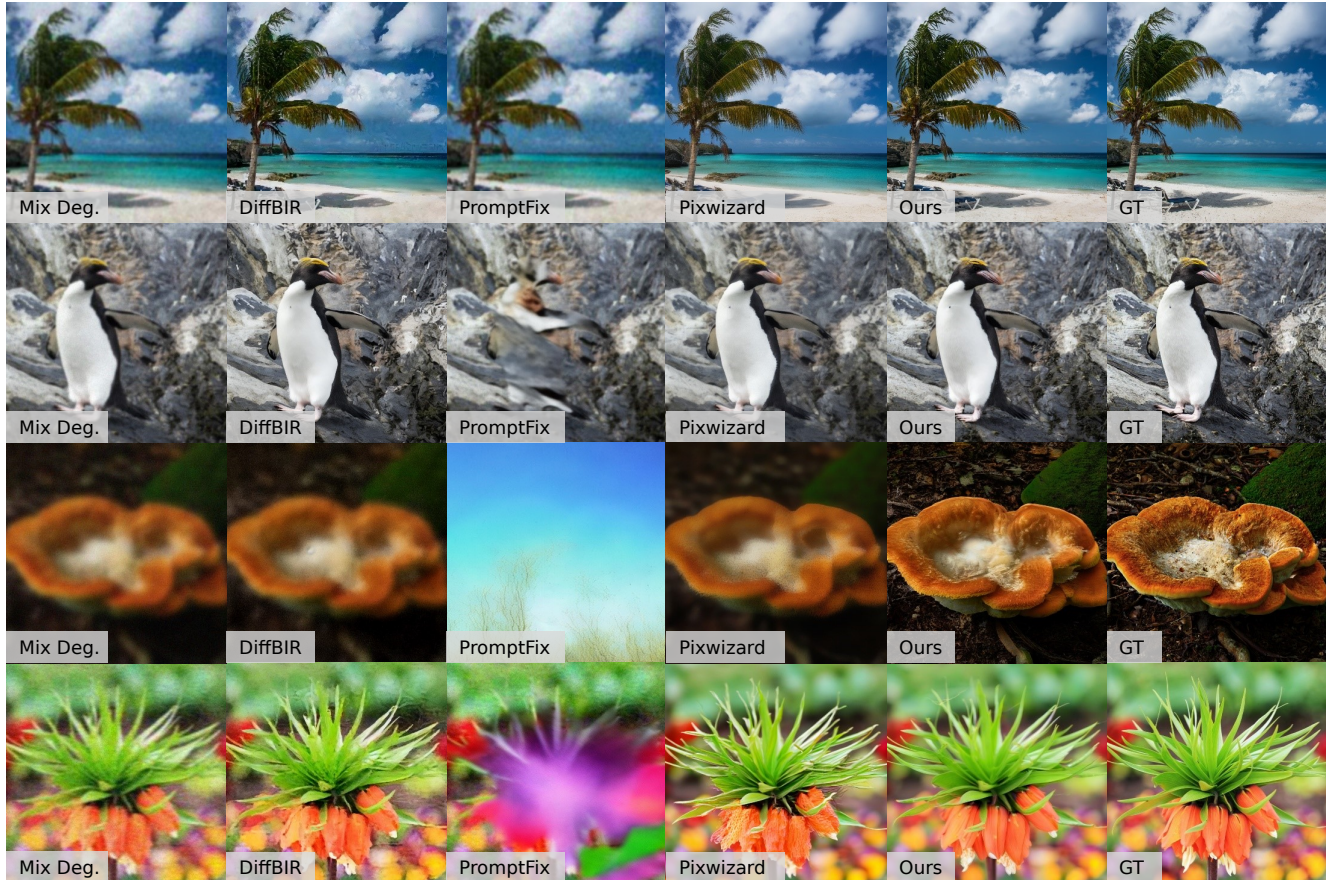


Figure 21. More results of mixed degradation restoration.

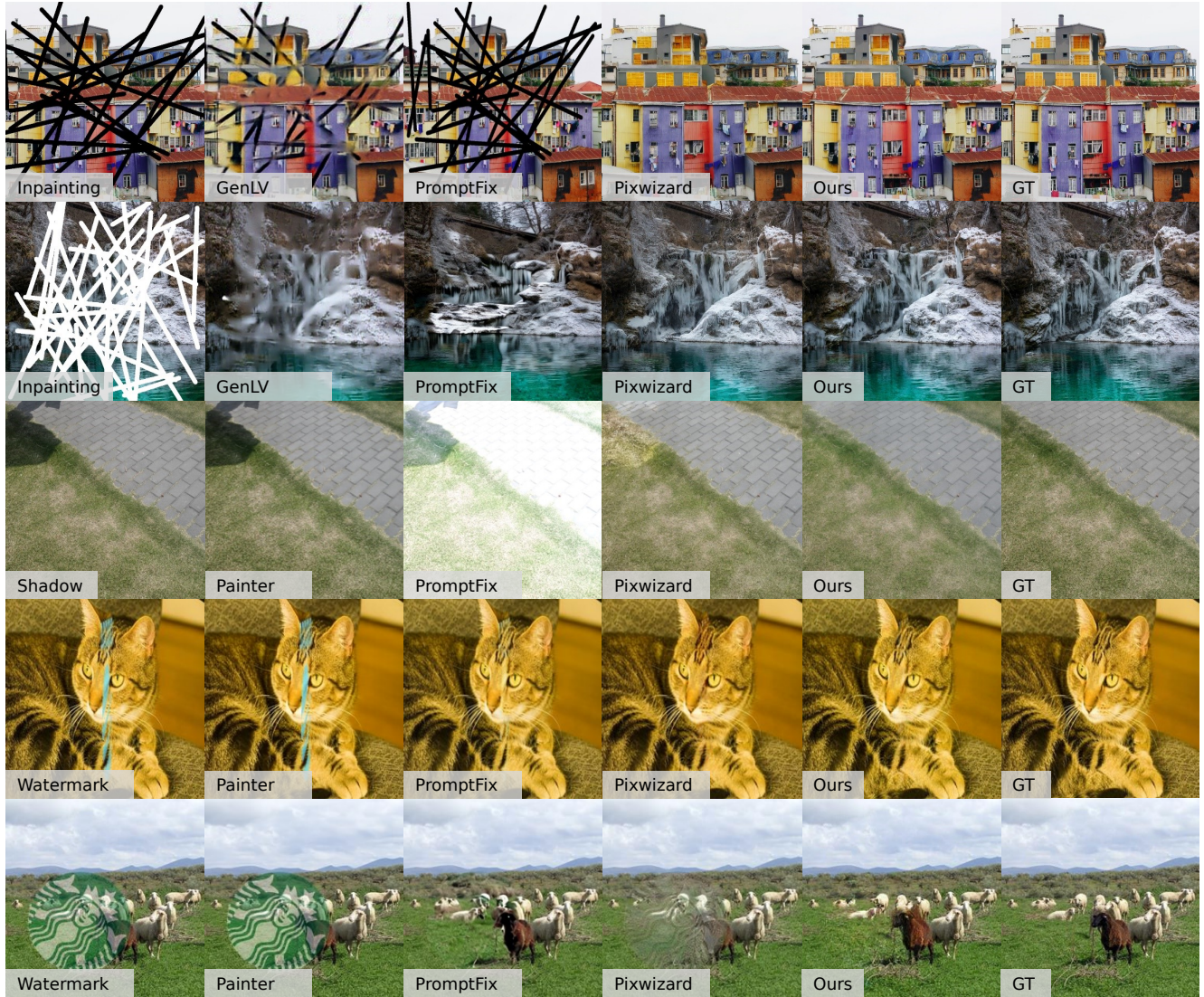


Figure 22. More results of image restoration.

Category	Method	Blur_Gaussian				Blur_Glass				Blur_Motion				Compression_JPEG			
		PSNR	SSIM	FID	MUSIQ	PSNR	SSIM	FID	MUSIQ	PSNR	SSIM	FID	MUSIQ	PSNR	SSIM	FID	MUSIQ
Specialized Models	XRestorer	23.34	0.6375	63.75	27.99	22.4	0.6187	80.1	28.71	19.42	0.5485	28.96	61.81	/	/	/	/
	MPRNet	23.28	0.6309	69.91	27.14	21.65	0.5884	80.55	30.58	19.73	0.5673	28.46	59.06	/	/	/	/
All-in-One Restoration	MAXIM	23.32	0.6353	70.24	26.53	22.26	0.6102	77.62	29.52	19.7	0.5634	30.38	58.4	/	/	/	/
	X-Restorer	23.5	0.6429	65.13	27.86	21.16	0.5828	80.4	28.17	20.3	0.5961	50.25	42.8	/	/	/	/
Text-Prompt-based	DA-CLIP	19.39	0.5306	75.38	32.24	21.02	0.5837	83.38	29.22	19.63	0.5665	64.25	36.67	/	/	/	/
	AutoDIR	24.01	0.6712	43.38	46.35	19.28	0.5467	79.28	35.7	18.77	0.5452	37.98	47.88	/	/	/	/
Visual-Prompt-based	GenLV	24.11	0.6652	51.4	32.99	22.32	0.6172	73.08	30.96	20.72	0.5897	64.54	31.81	23.85	0.6861	66.7	36.43
	PromptGIP	21.1	0.5552	128.6	31.04	20.81	0.5523	147.4	31.93	19.01	0.5184	165.7	30.52	22.33	0.6096	93.84	36.89
Text-Prompt Based	Painter	16.84	0.4638	166.9	25.03	16.8	0.4808	166.8	27.4	16.53	0.4668	138.3	29.53	20.93	0.6405	97.07	38.4
	Prompt-Diffusion	9.339	0.2591	174.5	49.93	9.389	0.2406	168.4	56.39	9.446	0.2502	164.1	56.75	9.71	0.2433	154.5	62.26
Multi-Modal Based	Instruct-Pix2Pix	16.22	0.4955	127.6	34.46	16.04	0.4778	119.9	37.34	15.88	0.4658	112.3	37.93	16.53	0.4864	97.8	46.43
	MGE	17.59	0.5004	110	27.12	16.23	0.4424	134.3	32.89	15.06	0.4297	111.6	36.79	16.39	0.4912	118.1	51.46
Multi-Modal Based	PromptFix	24.48	0.7217	78.13	33.05	22.22	0.6649	99.78	40.05	20	0.6149	89.82	46.47	15.96	0.5802	187.1	58.75
	PixWizard	20.49	0.5367	59.23	67.66	19.65	0.5162	59.58	65.54	17.42	0.4763	64.04	65.15	18.81	0.53	63.87	60.02
Multi-Modal Based	Omniv	23.29	0.6437	18.19	67.98	22.41	0.6299	25.43	68.45	23.36	0.6697	16.73	69.4	23.79	0.6854	29.05	69.12

Table 8. Restoration results.

Category	Method	Noise_Gaussian				Noise_Poisson				Pixelate				Quantization_Hist			
		PSNR	SSIM	FID	MUSIQ	PSNR	SSIM	FID	MUSIQ	PSNR	SSIM	FID	MUSIQ	PSNR	SSIM	FID	MUSIQ
Specialized Models	XRestorer	27.37	0.7856	40.85	68.27	29.52	0.8603	45.46	69.24	/	/	/	/	/	/	/	/
	MPRNet	23.67	0.6909	65.67	43.58	25.81	0.7714	40.49	49.86	/	/	/	/	/	/	/	/
All-in-One Restoration	MAXIM	22.88	0.6959	68.16	46.89	26.35	0.7938	44.97	54.66	/	/	/	/	/	/	/	/
	X-Restorer	27.51	0.8022	23.94	69.65	28.63	0.8232	16.94	69.01	/	/	/	/	/	/	/	/
Text-Prompt-based	DA-CLIP	23.16	0.5769	70.62	45.54	23.19	0.5821	61.6	43.08	/	/	/	/	/	/	/	/
	AutoDIR	26.78	0.7882	20.34	60.15	28.23	0.8559	12.61	63.12	/	/	/	/	/	/	/	/
Visual-Prompt-based	GenLV	23.1	0.6406	79.11	38.48	23.91	0.6938	60.56	39.65	24.28	0.6977	33.97	36.89	21.83	0.6701	66.33	37.99
	PromptGIP	22.54	0.6046	84.05	35.32	22.98	0.6389	72.32	35.69	22.01	0.6025	92.48	34.61	15.1	0.5046	159.4	35.37
Text-Prompt Based	Painter	17.56	0.5603	123.5	36.22	16.96	0.5531	132.7	38.34	18.43	0.553	110.6	36.02	12.5	0.4319	186.6	34.92
	Prompt-Diffusion	9.779	0.2199	160.3	60.41	9.79	0.2383	154.2	62	9.689	0.2587	153.4	61.77	9.18	0.2455	155.7	63.33
Multi-Modal Based	Instruct-Pix2Pix	14.7	0.3935	114.2	46.8	15.28	0.4316	101.1	48.5	15.69	0.4556	90.6	56.01	14.15	0.4504	98.8	47.22
	MGE	14.47	0.2379	121	40.99	15.7	0.3078	92.45	48.28	13.9	0.3517	172.7	49.02	12.9	0.3921	118.3	58.23
Multi-Modal Based	PromptFix	13.99	0.4334	207.2	50.08	15.16	0.523	185.8	55	18.34	0.6494	143.6	59.09	12.51	0.543	193.6	59.29
	PixWizard	17.05	0.434	74.85	62.13	15.8	0.4423	76.09	62.52	14.31	0.4422	103.4	57.6	13.98	0.456	86.58	65.38
Multi-Modal Based	Omniv	23.21	0.6405	26.17	69.78	23.98	0.6778	19.3	69.82	23.45	0.6673	16.7	68.5	20.46	0.6457	33.85	69.46

Table 9. Restoration results.

Category	Method	Quantization						Otsu						Ringing					
		Median	FID	MUSIQ	PSNR	SSIM	FID	MUSIQ	PSNR	SSIM	FID	MUSIQ	PSNR	SSIM	FID	MUSIQ	PSNR	SSIM	
Specialized Models	XRestorer	/	/	/	/	/	/	/	/	27.1	0.8691	45.87	71.34	/	/	/	/	/	
	MPRNet	/	/	/	/	/	/	/	/	25.16	0.8397	64.83	69.4	/	/	/	/	/	
	MAXIM	/	/	/	/	/	/	/	/	25.82	0.8537	55.18	71.15	/	/	/	/	/	
All-in-One Restoration	X-Restorer	/	/	/	/	/	/	/	/	23.28	0.7832	91.22	69	/	/	/	/	/	
	DA-CLIP	/	/	/	/	/	/	/	/	23.15	0.7231	58.17	53.18	/	/	/	/	/	
	AutoDIR	/	/	/	/	/	/	/	/	25.33	0.8104	42.63	64.59	/	/	/	/	/	
	GenLV	22.19	0.6725	84.79	35.59	20.83	0.6684	69.59	38.31	21.05	0.6146	107.1	36.43	25.1	0.7266	34.04	39.28		
Visual-Prompt-based	PromptGIP	21.25	0.5963	116.4	34.35	17.87	0.5464	129.5	35.73	21.17	0.5868	100.5	34.25	23.34	0.6488	60.82	35.76		
	Painter	16.31	0.5247	153	36.33	14.29	0.4893	174.7	36.73	22.48	0.6649	74.64	41.3	16.16	0.5224	159.4	37.51		
	Prompt-Diffusion	9.508	0.2554	152.3	63.32	9.399	0.2488	150.9	63.76	9.743	0.1959	205.7	58.65	9.735	0.2703	147.9	63.23		
	Instruct-Pix2Pix	16.94	0.5018	91.1	49.15	15.37	0.4445	96.42	48.65	14.07	0.3412	173.6	42.28	16.76	0.5076	81.44	49.66		
Text-Prompt Based	MGIE	14.88	0.4414	98.6	59.51	14.3	0.4157	109.3	58.08	14.15	0.3252	200.6	54.41	15.96	0.4654	122.4	53.27		
	PromptFix	16.01	0.6116	182.1	59.56	14.36	0.5616	172.8	61.06	11.69	0.3404	246.6	57.63	18.22	0.6788	161.6	61.62		
	PixWizard	15.39	0.4769	76.05	65.62	15.2	0.4637	78.45	65.69	17.61	0.5003	64.05	70.66	21.55	0.6188	35.08	65.14		
Multi-Modal Based	OmniLV	22.26	0.6758	32.54	69.68	19.75	0.6428	35.88	69.35	23.23	0.6751	24.19	70.45	24.98	0.7268	11.51	69.74		

Table 10. Restoration results.

Category	Method	Spatter						SRx2						SRx4					
		PSNR	SSIM	FID	MUSIQ	PSNR	SSIM	PSNR	SSIM	FID	MUSIQ	PSNR	SSIM	PSNR	SSIM	FID	MUSIQ		
Specialized Models	XRestorer	/	/	/	/	19.45	0.6572	29.84	68.14	26.19	0.8127	9.401	69.39	/	/	/	/		
	MPRNet	/	/	/	/	/	/	/	/	/	/	/	/	/	/	/	/		
	MAXIM	/	/	/	/	/	/	/	/	/	/	/	/	/	/	/	/		
All-in-One Restoration	X-Restorer	/	/	/	/	29.29	0.9021	1.525	63.99	24.97	0.729	21.64	38.38	/	/	/	/		
	DA-CLIP	/	/	/	/	/	/	/	/	/	/	/	/	/	/	/	/		
	AutoDIR	/	/	/	/	28.58	0.8738	4.242	57.54	24.51	0.7214	21.37	47.27	/	/	/	/		
	GenLV	20.45	0.5752	130.9	36.4	25.67	0.7529	18.78	40.32	25.04	0.707	31.85	35.15	/	/	/	/		
Visual-Prompt-based	PromptGIP	20.69	0.5647	116.2	35.02	23.41	0.6585	56.96	36.74	22.53	0.6121	98.22	35.47	/	/	/	/		
	Painter	18.76	0.5392	134	39.12	15.37	0.5116	152.9	38.66	14.19	0.4348	187.6	33.13	/	/	/	/		
	Prompt-Diffusion	9.458	0.1922	185.7	9.681	0.2657	147.4	63.4	9.546	0.257	153	60.75	/	/	/	/	/		
	Instruct-Pix2Pix	15.47	0.3732	140	44.72	17.15	0.5187	78.82	50.06	16.95	0.5125	87.37	43.09	/	/	/	/		
Text-Prompt Based	MGIE	12.14	0.2523	214.4	57.58	12.68	0.3487	155.3	54.03	16.8	0.5086	99.93	42.7	/	/	/	/		
	PromptFix	14.69	0.4519	215	59.33	28.36	0.8741	65.52	68.68	28.03	0.873	30.8	54.87	/	/	/	/		
	PixWizard	16.87	0.4489	93.42	68.56	19.35	0.6113	36.45	66.59	21	0.5768	32.65	67.59	/	/	/	/		
Multi-Modal Based	OmniLV	23.4	0.6696	24	70.13	25.33	0.7371	10.4	69.65	24.08	0.687	12.88	69.09	/	/	/	/		

Table 11. Restoration results.

Category	Method	Brighten_Gamma			Brighten_Shift			Contrast_Strength			Contrast_Weaken						
		PSNR	SSIM	FID	MUSIQ	PSNR	SSIM	FID	MUSIQ	PSNR	SSIM	FID	MUSIQ	PSNR	SSIM	FID	MUSIQ
Specialized Models	RetinexFormer	/	/	/	/	/	/	/	/	/	/	/	/	/	/	/	/
	MPRNet	/	/	/	/	/	/	/	/	/	/	/	/	/	/	/	/
	MAXIM	/	/	/	/	/	/	/	/	/	/	/	/	/	/	/	/
	X-Restorer	/	/	/	/	/	/	/	/	/	/	/	/	/	/	/	/
	DA-CLIP	/	/	/	/	/	/	/	/	/	/	/	/	/	/	/	/
All-in-One Restoration	AutoDIR	/	/	/	/	/	/	/	/	/	/	/	/	/	/	/	/
	GenLV	21.03	0.6866	41.58	40.81	21.92	0.704	43.45	40.11	21.35	0.6561	62.12	37.91	22.8	0.7091	38.05	40.58
	PromptGIP	16.76	0.5732	81.93	37.36	15.69	0.5436	87.07	34.04	16.13	0.5214	129.7	34.65	18.49	0.5841	104.4	33.81
	Painter	12.6	0.4888	155.8	37.55	12.4	0.5071	144.8	37.21	10.73	0.3605	234.9	32.25	15.38	0.5335	71.47	40.01
	Prompt-Diffusion	9.402	0.254	149.9	62.77	9.41	0.2531	149.1	63.08	9.503	0.2345	156.4	62.51	9.51	0.251	156.1	63.87
Visual-Prompt-based	Instruct-Pix2Pix	13.91	0.4975	84.05	50.29	12.76	0.4759	88.31	48.94	13.3	0.4043	102.8	46.9	15.33	0.5022	86.52	54.06
	MGE	14.86	0.5232	72.61	64.43	14.58	0.5208	65.75	62.77	12.54	0.3478	114.5	57.9	15.13	0.5081	73.18	64.48
	PromptFix	11.25	0.5163	203.3	58.17	10.27	0.4747	210.6	57.62	10.45	0.3942	223.8	56.82	12.95	0.5209	190	57.51
	PixWizard	10.97	0.4895	87.31	64.77	11.39	0.5015	82.71	63.5	13.12	0.4472	76.24	64.76	14.76	0.4805	77.79	66.98
	OmniLY115k	23.08	0.7321	15.12	70.69	22.84	0.7145	16.57	70.36	21.89	0.6635	32.22	70.24	23.58	0.7261	14.02	70.57

Table 12. Enhancement results.

Category	Method	Darken_Gamma			Darken_Shift			Mosaic			Oversharp					
		PSNR	SSIM	FID	MUSIQ	PSNR	SSIM	FID	MUSIQ	PSNR	SSIM	FID	MUSIQ			
Specialized Models	RetinexFormer	15.81	0.61	58.85	66.74	17.93	0.6351	52.29	66.14	—	—	—	—			
	MPRNet	16.89	0.6916	47.41	67.45	16.28	0.6362	58.29	65.82	—	—	—	—			
	MAXIM	17.57	0.7467	39.88	69.54	14.41	0.621	63.38	66.54	—	—	—	—			
	X-Restorer	—	—	—	—	—	—	—	—	—	—	—	—			
	DA-CLIP	14.97	0.5477	45.75	55.05	15.58	0.5589	41.86	54.15	—	—	—	—			
All-in-One Restoration	AutoDIR	15.62	0.6709	38.28	66.44	14.19	0.613	38.8	67.11	—	—	—	—			
	GenLV	21.77	0.6865	44.23	40.15	21.92	0.6672	57.46	39.39	13.46	0.5118	203.7	36.09	21.69	0.6482	113.2
	PromptGIP	18.26	0.5605	110.9	34.57	18.28	0.5455	114.2	35.14	16.93	0.5388	194.5	32.68	20.7	0.6099	101.4
	Painter	13.73	0.4745	171.8	37.91	13.82	0.4633	177.1	36.98	15.08	0.5887	129.3	42.24	12.73	0.4351	201.3
	Prompt-Diffusion	9.323	0.2292	152.1	61.59	9.18	0.2274	159.4	60.9	9.636	0.1344	246.5	55.73	9.721	0.2542	146.7
Visual-Prompt-based	Instruct-Pix2Pix	13.15	0.3828	89.77	50.56	13.11	0.3787	88.11	50.5	11.21	0.3799	118.4	51.04	15.69	0.4556	90.6
	MGE	15.42	0.4745	68.78	63.07	15.28	0.4642	74.68	62.25	9.747	0.1919	241.7	53.35	13.53	0.346	114.1
	PromptFix	10.39	0.3981	212.8	54.75	10.63	0.4245	206.6	56.21	9.263	0.384	192.8	52.81	14.93	0.5861	170.7
	PixWizard	13.85	0.4452	75.34	65.44	14.3	0.4532	71.82	66.26	12.43	0.3345	127.7	63.24	13.55	0.4328	75.81
	OmniLY115k	21.08	0.6821	20.92	70.25	20.38	0.6597	28.22	69.79	23.93	0.7061	18.92	69.68	24.15	0.7188	17.7

Table 13. Enhancement results.

Category	Method	Saturate_Strength				Saturate_Strength				Saturate_Weaken				Saturate_Weaken			
		PSNR	SSIM	FID	MUSIQ	PSNR	SSIM	FID	MUSIQ	PSNR	SSIM	FID	MUSIQ	PSNR	SSIM	FID	MUSIQ
Specialized Models	RetinexFormer	/	/	/	/	/	/	/	/	/	/	/	/	/	/	/	/
	MPRNet	/	/	/	/	/	/	/	/	/	/	/	/	/	/	/	/
	MAXIM	/	/	/	/	/	/	/	/	/	/	/	/	/	/	/	/
All-in-One Restoration	X-Restorer	/	/	/	/	/	/	/	/	/	/	/	/	/	/	/	/
	DA-CLIP	/	/	/	/	/	/	/	/	/	/	/	/	/	/	/	/
	AutoDIR	/	/	/	/	/	/	/	/	/	/	/	/	/	/	/	/
	GenLV	21.52	0.6972	62.83	40.74	17.45	0.6393	67.72	39.39	22.16	0.7108	53.29	40.42	22.34	0.7123	53.33	40.57
Visual-Prompt-based	PromptGIP	13.6	0.4497	176.1	32.26	14.54	0.4795	182.8	33.65	19.01	0.5878	140	36.02	19.35	0.5982	156.1	35.99
	Painter	10.8	0.3759	213.8	35.08	10.97	0.3896	221.7	34.21	15.34	0.567	134.4	38.71	15.88	0.5673	146.1	38.6
	Prompt-Diffusion	9.257	0.2458	154.2	63.56	9.101	0.2431	156.3	63.65	9.273	0.2497	154.6	63.33	9.39	0.2575	157.2	62.87
	Instruct-Pix2Pix	12.49	0.3813	11.57	50.03	12.4	0.4078	11.74	49.7	16.38	0.5168	83.61	50.96	16.76	0.5218	90.73	51.85
Text-Prompt Based	MGE	12.31	0.3957	108.7	58.81	11.67	0.3831	128.5	57.69	15.23	0.5168	78.96	63.05	15.43	0.5255	90.48	62.53
	PromptFix	10.41	0.4065	221.1	56.3	10.49	0.4137	230.8	58.3	13.73	0.5779	182.5	59.53	14.59	0.5975	175.1	59.81
	PixWizard	12.78	0.4177	96.79	63.84	12.09	0.4374	102.2	64.13	12.76	0.5243	91.76	65.75	13.41	0.5287	90.64	66.78
Multi-Modal Based	Omnily115k	20.91	0.6531	37.98	70.77	21.7	0.6762	35.61	71.16	22.15	0.7106	25.68	70.93	22.4	0.7149	33.78	70.74

Table 14. Enhancement results.